Hervas-Blasco, E.; Navarro-Peris, E.; De Rosa, M.; Corberán, JM. (2017). Potential fuel saving in a powertrain derived from the recovery of the main energy losses for a long haul European mission. Energy Conversion and Management. 150:485-499. doi:10.1016/j.enconman.2017.08.018

Potential fuel saving in a powertrain derived from the recovery of the main energy losses for a long haul European mission.

Estefanía HERVAS-BLASCO[(a)], Emilio NAVARRO-PERIS[(a)*], Mattia DE ROSA[(b)], José M. CORBERÁN[(a)]

[(a)] Instituto Universitario de Investigación en Ingeniería Energética (IUIIE), Universitat Politècnica de València, Camí de Vera s/n, Valencia, 46022, Spain.

[(b)] School of Mechanical and Aerospace Engineering, Queen's University Belfast. Ashby Building, Stranmillis Road, BT9 5AH, Belfast. United Kingdom.

ABSTRACT

The reduction of automotive fuel consumption and emissions remains one of the main challenges. This paper presents the potential fuel saving in a CNG-powertrain derived from the recovery of the main energy losses. The analysis includes the kinetic energy recovery by a belt starter generator (BSG), the exhaust gas waste heat recuperation by using in a cascade approach, a thermoelectric generator (TEG) and a turbo-generator (TBG)- and the electrification of the main auxiliaries. An additional 48V board net as well as the addition of a storage system are also included in the study. To support on the design phase of the project and in the operation strategy, a dynamic model in Matlab/Simulink® has been used. The model includes all the new components/major changes required in the vehicle- experimentally validated-. It has been used on backward simulations for the ACEA long haul mission in order to maximize the vehicle's efficiency.

Estimations at rating point (600Nm and 1200rpm) result in an electric production up to 4 kWh and a fuel saving of 7.5%. The most convenient technologies in the ACEA cycle turns out to be the KERs followed by the TBG.

Keywords: modelling, efficiency, energy recovery, optimal control strategy, powertrain, fuel saving

*Corresponding author: Emilio Navarro-Peris, emilio.navarro@iie.upv.es, Tel: +34 963879123

1.- Introduction

Transport sector accounts for more than 25% of the total world's energy consumption and 23% of it is occasioned by heavy duty trucks with a growing perspective future share [1]. Under the purpose to reduce emissions, policies oriented to lower fuel consumption and emissions are being imposed worldwide [2] leading to a technology evolution towards a higher vehicle efficiency and the use of alternative fuels [3].

In this transport sector, the use of Compressed Natural Gas (CNG) is being one of the most suitable option as cleaner alternative fuel due to its availability and characteristics [4] .

In CNG long distance vehicles, only around 40% of the total available energy from the fuel is actually used for motion purposes and its efficiency is reaching its physical limit [5]. The rest is either waste as heat to the ambient (1/3 through the exhaust system and around 15% to the cooling circuit [5]) or lost between the different heat exchange processes (oil, charge air (compressed air), lubricating…) as can be seen in Figure1.

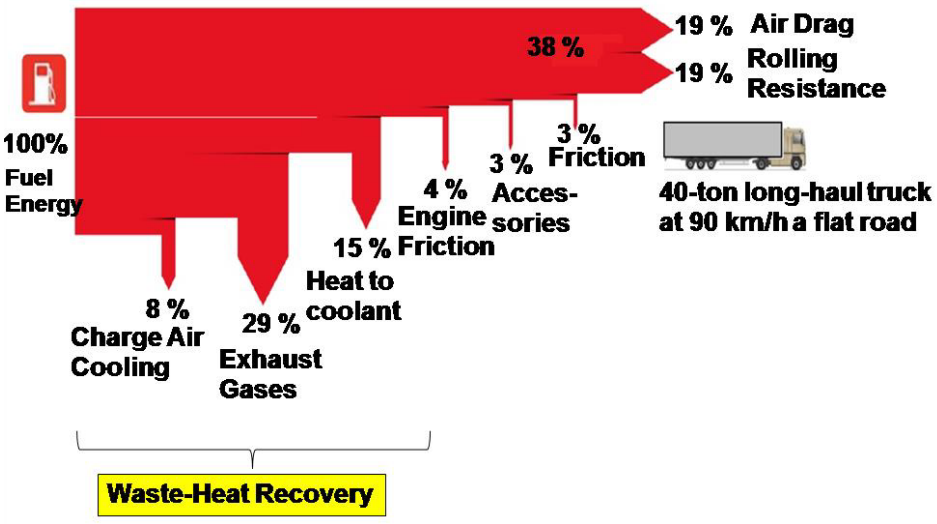

Figure 1: Energy flow for a long distance CNG engine vehicle [6].

Nonetheless, this significant amount of waste energy is of low quality, as its low exergy limits its complete recovery [7]. Among all the losses stated in figure 1, the exhaust gases waste energy is the most important source of losses. In addition, its high temperature compared to the rest of the losses make this, the most useful waste source [8]. In fact, the development and application of new technologies to efficiently recover it, has been a major global concern as it can be seen in [9]

and [10]. Moreover, among the commonly fuel engines, CNG engines present the higher exhaust gas temperatures. Therefore, Natural Compressed Gas engine has been chosen for the application considered in this study.

Despite the big gap of improvement available in the energy waste flows of an engine, most of the previous engine's improvement consider only single/few isolated technologies [11]. In fact, there is an extensive literature in which the most common technology used to recover exhaust heat is the Organic Rankine Cycle (ORC) as it can be seen in a feasibility analysis of this type of systems in [12], in a test bench for different combustion engines in [13], for passenger cars in [14] OR in [15] for heavy duty trucks where 2% of improvement is attained by the introduction for ORC. Moreover, it is easy to find analysis about the potential improvement by the addition of electric turbochargers [16] and in passenger cars [17], thermoelectric generators (TEG) within automobile sector[18], in heavy duty vehicles [19] or modeling analysis of its performance in [20] and Kinetic energy recovery systems (KERs). However, much less studies have been carried out with the use of Turbo-generators (TBG) [21] even though this mature technology has a great potential [22]. Most of them are based on individual approaches so they may miss the best potential of a technology that could come from the combination and proper operating strategy definition based on the consideration of different possibilities/technologies/solutions. In fact, the biggest advantage of the introduction of new technologies could rely on the coupling of the whole system for a target application (driving cycle).

The improvement by means of modifications in the existing components and/or the addition of new technologies only can be optimized when is coupled with the final target driving cycle according to [23] or [24] where various driving cycles are analyzed, the type of engine [25] and with the definition of proper control strategies [26].

Hence, the use of dynamic models that are able to reproduce the real behavior of the vehicle taking into account all the interactions and possibilities among the different components, becomes a very useful tool [27] that can support in the development of the most convenient solution.

Commercial software in the automotive field are very common and used by the main OEMs of different vehicle's types with purposes similar to these (GT-powers, AVL packages…)[28]. In fact, they are very useful to perform standard simulations but none of them had the possibility to integrate all the new features of the case study presented in this work by default [29]. Therefore, a new dynamic model using Matlab/Simulink in order to analyze non standard solutions has been developed. This model could be, at the end, coupled to the previous cited software.

This work presents the analysis of the most attractive operational strategy and the estimation of the potential fuel saving derived from the simultaneous use of several recovery technologies in a CNG powertrain based on simulation results. The followed approach is based on the recovery of waste energy from different sources (kinetic and heat) in order to generate electric energy that is stored for a latter consumption. Thus, a reduction on the fuel consumption is possible, on the one hand, thanks to the substitution of the belt-driven alternator, the mechanical engine auxiliaries such as compressors, pumps and the like by electric auxiliaries (reducing the engine torque request as well as the mechanical friction losses). On the other hand, thanks to the adoption of an electric booster and the use of a water-cooled charge air cooler (allowing the control of the engine inlet conditions). These electric auxiliaries are fed by the electric energy generated through exhaust gas recovery systems and the kinetic energy recovery system by means of an optimized operating strategy of the storage system for the ACEA cycle. This case study considers a combination of technologies that has not been analyzed before [30]. Specifically, a TEG, a TBG and a KERs as electric generators and aims to study the potential improvement in the efficiency of a CNG engine in a long haul driving cycle.

The fuel consumption reduction analysis in heavy-duty powertrains by the recuperation of kinetic energy, the exhaust gas heat recovery and the reduction of friction losses at once employing the technologies proposed in this study (TEG, TBG and KERs) is a challenging proposal not available in literature yet and is analyzed in this work. A final sensitivity analysis including a Diesel engine is also considered.

2.- Model Concept

The model has been developed using the respective equations that reproduce the behavior of each component in the vehicle and it is implemented in Matlab-Simulink® software [31]. The use of this platform by the main manufacturers as well as its easy implementation allow its integration in other automotive specific platforms like Autonomie, GT-Suite or AVL packages [32].

The following parts of this section focus on the description of the main features included in the model presented in this work.

2.1. Model Structure

The model is composed by a modular structure based on experimental data with an error lower than 5% according to the model validation as it is shown in the Annex. Thus, the optimization not only of the isolated components but also of the overall system is possible.

- **Inputs of the model:** the main inputs are the ambient conditions, the water and air specific thermal capacities, the setting engine temperature, the inertias of the components, physical limitations of the different components (maximum/minimum operating temperatures and pressures) and the driving cycle (by means of engine speed, torque request, vehicle velocity and the deceleration periods).
- **Driving cycle:** Any type of cycle could be simulated and the optimal control strategy will depend on the application target. For this work, the ACEA driving cycle has been utilized. This cycle is considered as a representative cycle for a heavy duty trucks in the transportation sector within Europe [33]. Figure 2 shows the vehicle speed and the engine speed profiles while the engine torque profile can be seen in Figure 3.

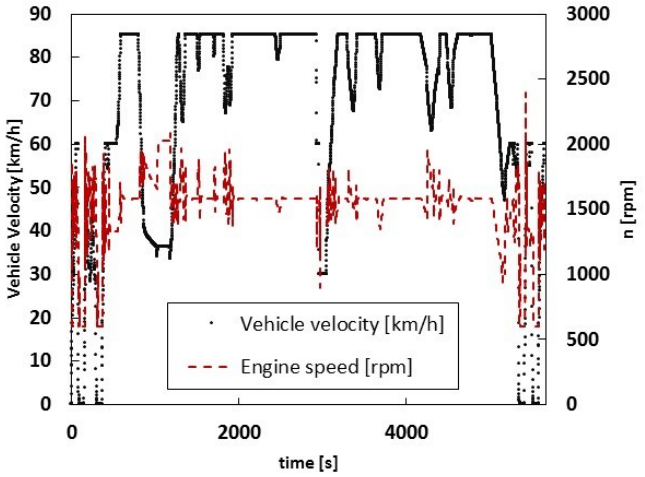

Figure 2. Vehicle speed [kmh^{-1}] and normalized engine speed profiles

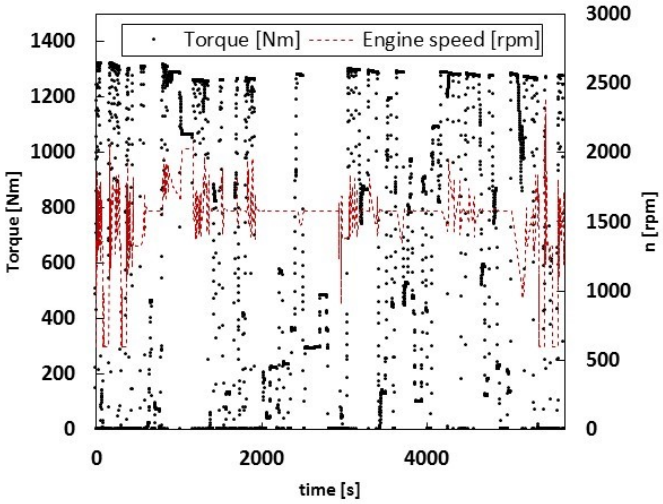

Figure 3. Engine torque and engine speed normalized profiles.

- **Outcome of the model:** the most important result from the model is the benefit. This benefit is expressed in terms of fuel saving and CO2 emissions reduction by the comparison of a reference vehicle (in this work: IVECO STRALIS CNG MY2014) together with a reference engine (in this work: Cursor8 CNG Euro VI) with a new powertrain concept which engine includes improvements explained afterwards. In addition to these benefit, all the thermal properties of the fluid along the whole system, the individual electric production/consumption, the energy balance, the battery level or the cooling circuits are also evaluated all along the driving cycle.

2.2. Energy recovery components included in the model

The basic approach followed in this work to recover the waste energy (from kinetic energy of the vehicle and exhaust gases) consists of generating electricity in order to use it to feed several vehicle accessories that were previously dependent on the mechanical energy of the engine. Thus, reducing the fuel consumption. Moreover, other approaches to make the engine operation more efficient like controlling the temperature of the compressed air at the inlet of the engine or introducing an electrical turbo are analyzed in this work.

2.2.1 Waste heat recovery

Basically, the more studied available technologies to recover waste energy from the exhaust gases are: TEG [30], ORC [34] and TBG [35]. In the proposed study, the thermoelectric and the turbocharger technologies are included.

2.2.2. Recovery of kinetic energy

The adoption of a KERs as an advanced starter generator is also included in the model. This system substitutes the alternator resulting in a reduction of the torque requested as well as of the friction and gear losses [36]. The control strategy employed has been determined based on the interaction between the rest of the components in order to maximize the fuel saving and ensure the electric service to the e-auxiliaries.

2.2.3. Electrification of the main auxiliaries, development of a storage system and optimal thermal and electric control strategies

The following auxiliaries have been considered in the vehicle: engine coolant pump, oil pump, steering pump, starter/generator, auxiliary e-booster, fan and AC compressor. The total energy requirements of them has been estimated in terms of mechanical torque value respectively. Based on the energy generated, the potential substitutions and saving derived from that are evaluated.

As the potential energy recovery could not meet at the same time with the auxiliaries' energy requirements, the design of an appropriate storage system to optimize the production and guarantee the electric supply has also been an aim of the model. An advanced 48-Volt board net architecture with central unit control to allow the optimized control of the system and power

electronics to run the electrified subsystems, storing the power as well as to handle the peak demands are also considered.

The thermal layout of the considered technologies in the model is represented in Figure 4. Red lines belong to the high temperature cooling circuit, blue lines to the low temperature cooling circuit, orange lines to electric connections, light grey to the air circuit and grey to the exhaust gas circuit.

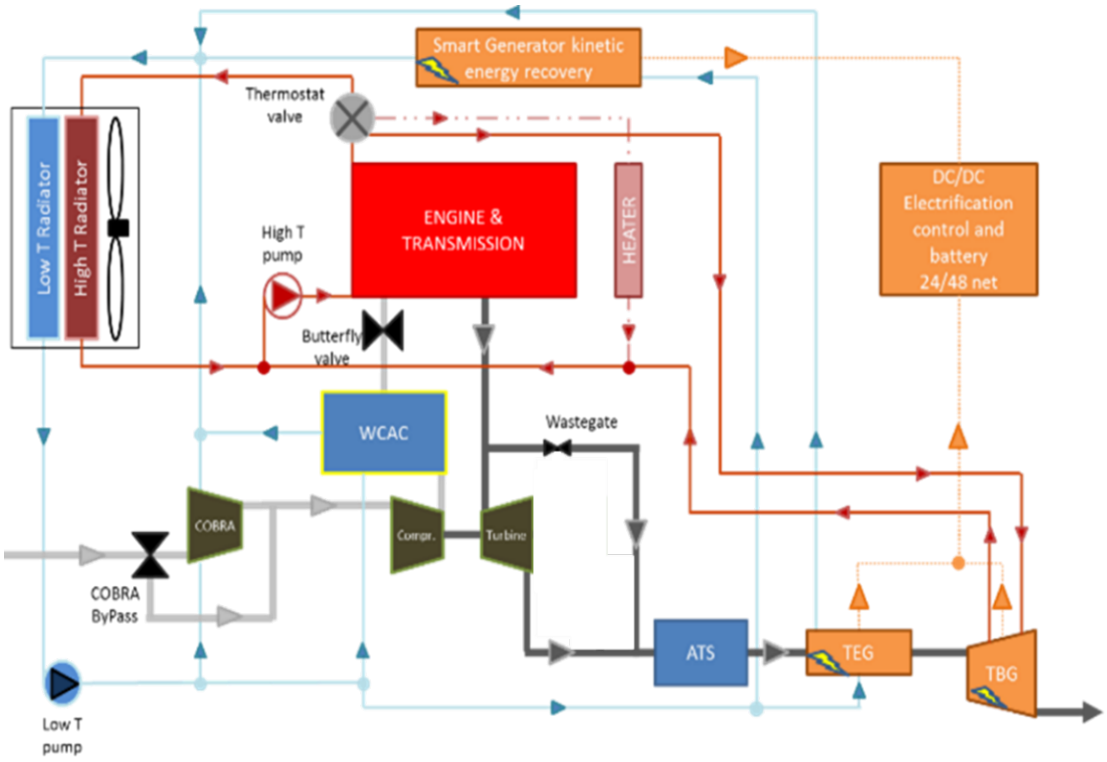

Figure 4: thermal layout

Figure 5 represents a flow diagram of the boxes that composed the model of the system.

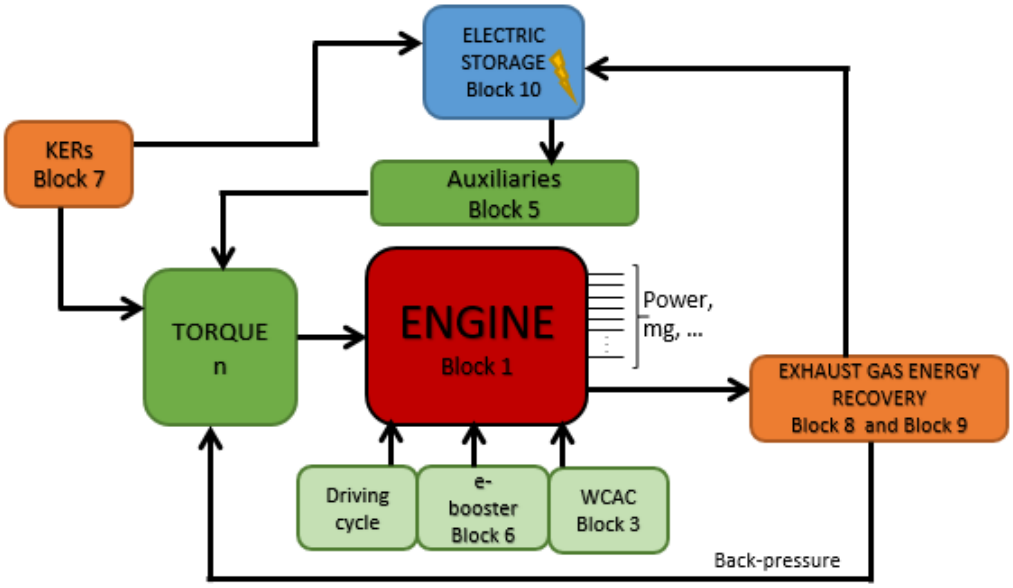

Figure 5: Flow diagram of the model

4. System model

The system model consists of 10 blocks-apart from the "input file and the results" block-connected among them. For further details regarding to mathematical equations, an Annex has been included.

Block 1: CNG gas engine

This is the core block. It contains the mathematical expressions correlated from the experimental data of the engine. All the equations are function of the torque and the engine speed. The main external inputs are the vehicle speed, the engine speed and the torque request. If other engine is considered, the correlations have to be redefined. Nevertheless, it has been performed also for a diesel engine relatively easily.

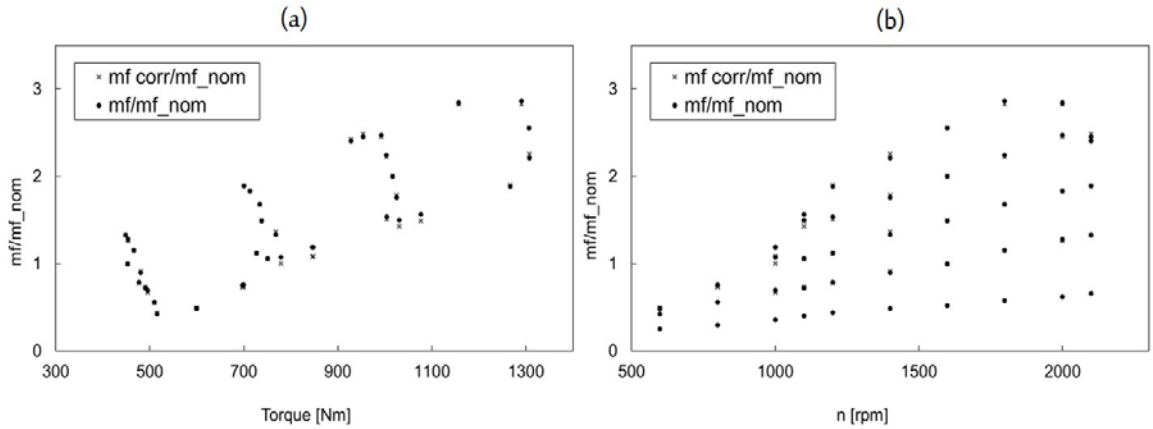

185

186 The electrification of the auxiliaries as well as the increase of the back-pressure by the additional
187 technologies included in the tailpipe of the exhaust gas circuit are accounted by a correction of
188 the torque from where every variable is then calculated according to the correlations function of
189 the torque and the engine speed. A reduction of the requested torque due to the electrification of
190 the main auxiliaries' equals to the mechanic torque request and an increase of it because of the
191 back-pressure effect by the additional new components downstream of the engine is done. The
192 fuel saving is calculated based on this torque correction for every specific period of the driving
193 cycle.

194 The outputs of this block are:

195 - Mechanical power
196 - Fuel consumption
197 - Gas mass flow rate
198 - Water mass flow rate through the high temperature cooling system
199 - The heat dissipated to the ambient
200 - The exhaust gas heat and temperature
201 - The heat dissipated to the radiator
202 - The available heat from the fuel

203 For both, the reference and the new concept vehicle.

204 Table 1 contains the main features of the reference the electrified engine considered in this work.

Table 1. Summary of the main engine and powertrain features

REFERENCE VEHICLE	NEW POWERTRAIN VEHICLE
Engine: Cursor8 CNG Euro VI	Engine: Cursor8 CNG Euro VI
Mechanic alternator	Kinectic Energy Recovery System
High temperature cooling circuit	Dual loop cooling circuits: high and low temperature circuits
High temperature radiator	High and low temperature radiators
Mechanic water pump, oil pump and steering pump	Electric water pumps, oil pump and steering pump
Air cooler	Water Cooled Charge Air Cooler
Turbo-compressor	Turbo-compressor + e-booster
	Exhaust gas recovery syst: TEG+TBG
	Dual voltage boardnet
	Energy storage system

Block 2: High temperature cooling circuit

This block contains the mechanical pump model, the electric pump model and the addition of the turbo generator to the cooling circuit.

Figure 6 is the high temperature cooling circuit reduced layout. The main differences respect to the reference vehicle is the addition of a parallel circuit to handle the TBG cooling, the electric water pump and the placement of the radiator in parallel with the low temperature radiator. Moreover, the electric water pump allows optimizing the water mass flow rate in order to maintain a set temperature at the outlet of the engine in every period. Thus, being able to actuate independently of the mechanic engine.

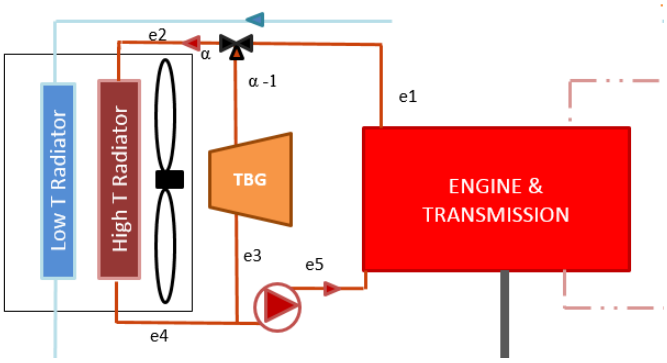

Figure 6. High temperature cooling circuit modified and radiators layout

This blocks contains, in addition, the modelling of both radiators according to the expressions detailed in the Annex.

The e values represent each state of the high temperature cooling circuit while the α is the aperture of the valve of the thermostat.

The inputs are: the mechanical water mass flow rate, the vehicle speed, the engine initial temperature, the engine setting point and the heat dissipated in the TBG (according to manufacturer specifications) and the high temperature radiator.

The outputs are: the outlet water temperature of the radiators, of the engine and of the TBG, as well as the water mass flow rate in the electric pump.

Block 3: Low temperature cooling circuit

An additional low temperature cooling circuit with an electric pump is required in order to ensure the proper cooling down of all the recovery systems (TEG, KERs, WCAC, the DCDC and the e-booster). The radiator is placed in parallel to the high temperature radiator.

In this case, the control parameter is the water mass flow rate in order to maintain the water working temperature within the specified range of every component considering the most critical point the outlet water temperature of the TEG (that must be between 20-45ºC in order to avoid the damage of the cartridges and to ensure its maximum power production). Therefore, this water mass flow rate is regulated by the electric water pump based on the set temperatures. According to the most realistic design, the final layout has been decided to be the placement of all the components in parallel as it shows in Figure 7.

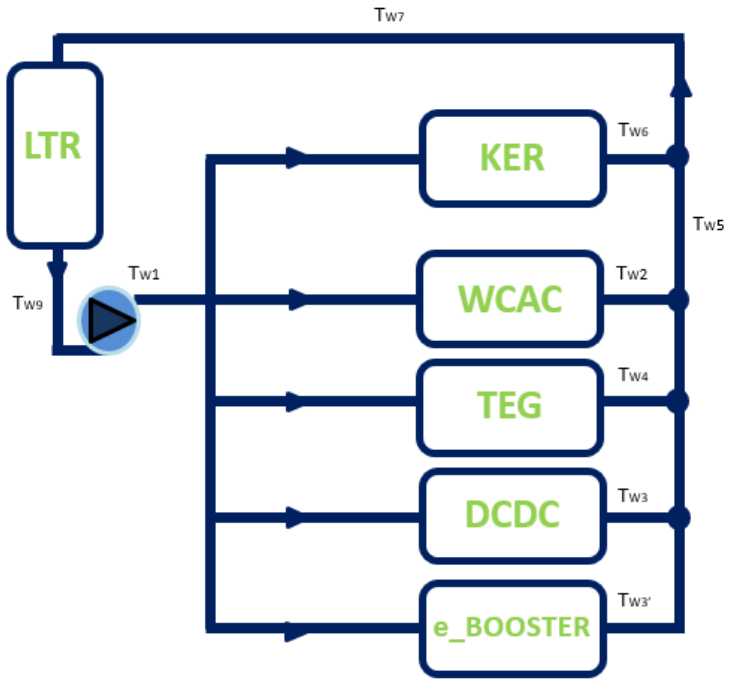

Figure 7. Low temperature cooling circuit layout

Where Twi represent the water temperature at the position "i" and the blue circle, the low temperature electric water pump.

The use of a Water Cooled Air Cooler instead of an Air Cooler allows the control of the inlet air temperature at the engine and its model follows the same approach as for the radiators just commented before.

Finally, the inputs of this block are: the water mass flow rate through the components and the heat dissipated in the correspondent components. While the outputs are the temperatures at any point of this subsystem.

Block 4: Water pumps

This block is included, respectively, inside the two cooling circuits commented above. It focuses on the calculation of the water mas flow rates, the water pressure drops among the respective components and the electric consumption. Pipe circuits losses are accounted and the models of both electric pumps as well. Their models are based on mathematical expressions from experimental data of the components.

The inputs are of the low temperature water pump are: the temperature of the components. While the outputs are the consumption of the pump, the water mass flow rates through the components and the pressure drop.

Block 5: Electrified auxiliaries

The aim of this block is to calculate the mechanical power required by the reference mechanical components based on experimental data. Then, this power is expressed in terms of torque (by the engine speed relation). Afterwards, to take into account the benefit of its substitution, a reduction of the engine torque equals to the torque requested by the mechanical technology is applied to the engine. The electric consumption of the electrified auxiliaries is calculated from the models given by the respective manufacturer.

Inputs: engine speed and water mass flow rates. Output: respective torque decrease and electric consumption.

Block 6: e- turbo

An exhaustive study of this component and its optimal control strategy has been done. It is based on the engine map and the dependency of its performance with the inlet conditions in order to make it boost when most appropriate. To find more details about the modeling, please refer to the Annex.

The model given from the manufacturer has been coupled to the system model.

The inputs of this block are: the air mass flow rate and the pressure ratio while the outputs are the electric consumption and the e-booster speed.

Block 7: KER System

This is a wide used technology. An existing KER system has been utilized, the manufacturer has supplied a model for that device that has been integrated in the global model. The model includes the possibility for the KERs to work recuperating the kinetic energy and as a motor.

Inputs: deceleration periods, engine speed, motor mode electric production required.

Outputs: electric production, increase of the torque and the heat to dissipate.

Block 8: Thermo Electric Generator

The model is based on experimental correlations from a single cartridge based on the characteristic curves given from the manufacturer. Afterwards, a complete study was performed (taking into account space and temperature limit constraints) in order to define the optimal design as well as the optimal number of cartridges to use.

The final configuration as well as the validation of the model of the complete TEG is detailed in the Annex.

Finally, the back-pressure effect has been calculated and translated into a correction of the torque resulting in an additional consumption.

The inputs are: the water and gas mass flow rate, the water and exhaust gas inlet temperatures and the temperature limit.

The outputs are: the outlet water and gas temperatures, the electric production, the heat to dissipate and the torque increase due to the back-pressure effect.

Block 9: Turbo Generator

The model of this component is based on the basic mathematic equations for turbines and its inputs are the gas mass flow rate, the outlet pressure and the inlet temperature according to the maps given the manufacturer.

The main constraint in the electric production is the back-pressure. Several simulations demonstrated that values higher than 300mbar lead to a not profitable electric production (the final benefit decreases due to an increase of fuel consumption by the engine). Therefore, this is the control parameter that limits the electric production. A by-pass is also integrated in the system in order to avoid the over-production and damage.

The outputs of this block are: the electric production, the back-pressure, the outlet temperature and the inlet pressure.

Block 10: Storage system

This block contains the models of the battery (two 12V batteries in series) and the DCDC 48/24V converter that comprises the advanced energy storage system. Figure 8 represents the advanced energy storage system layout.

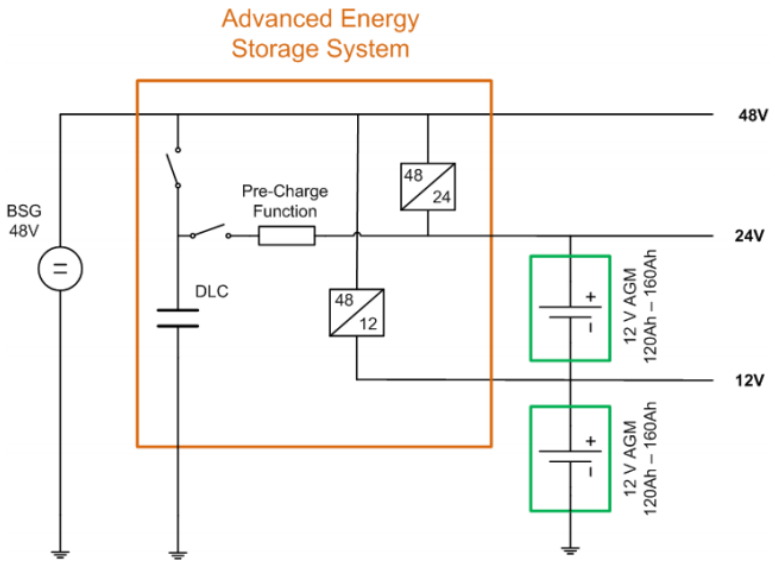

Figure 8. Advanced energy storage system layout.

The inputs are the electric consumption and production of all the components considered in the system, the initial state of charge and the main characteristics of the battery (for instance the capacitance, the resistance, the variation of the efficiency with the level of charge and the initial voltage) and the output is the final state of charge of the battery.

The modelling is based, first, on an electric balance between the 24V consumers (electrified auxiliaries and pumps) and producers (TEG) together with another balance for the 48V components (TBG, KERs). These are the inputs of the battery model.

On the one hand, the battery charges if the 24V power balance is greater than zero while discharges when the consumption becomes higher than the production. On the other hand, the 48V balance is converted to 24V with its respective efficiency charging or discharging.

Both models are directly related by the state of charge which is converted by interpolation within a map from the specifications of the component to a 24V signal and influences the possible 48V conversion.

The battery model outputs are the voltage of the double layer capacitor (DLC) regarding to the 48V part and the state of charge which also is afterwards translated into a 24V value. Both voltages signals are the inputs of the DCDC model. The outcomes of this model are the intensity of the 24V and 48V parts. Finally, both outputs feed the respective electric balances commented at the beginning of this block.

The main control is based on the state of charge of the battery. The objective is to be at the same level at the end of the cycle simulated as the initial level (set in this case to 50%). A PID control has been implemented and this level is reached at the end of the driving cycle by the regulation of the production of the KERs system out of deceleration periods. In addition, the level of the battery charge cannot be lower than 20% nor higher than 80%. The first value is a necessary safety decision in order to ensure the electric supply while values of the charge up to 80% shorten the life of the battery considerably (according to the component specifications given by the manufacturer).

5.-Results and Discussion

As it has been commented, apart from the fuel saving, the model is able to provide information about all the system variables. This fact allows a complete analysis of the system and its optimization. In this section, an example of results for a determined cycle extracted from the model are presented and from them a final estimation of the system potential and optimum system configuration is commented.

First, the model has been used in order to define and properly size the components. After, the optimization of the system for the specific target driving cycle is done. In the following results, the name “reference” refers to the reference vehicle and the “electrified” has been used for the

new concept vehicle which incorporates the electric auxiliaries as well as several energy recovery technologies.

Figure 9 shows the mechanical power [kW] and exhaust gas heat [kW] of the reference vehicle for the driving cycle. The figure allows to have an overall estimation of the magnitude order of the waste heat through the exhaust gas system compared to the mechanical power. That is, a general view of the available energy to be recovered by the TEG and the TBG.

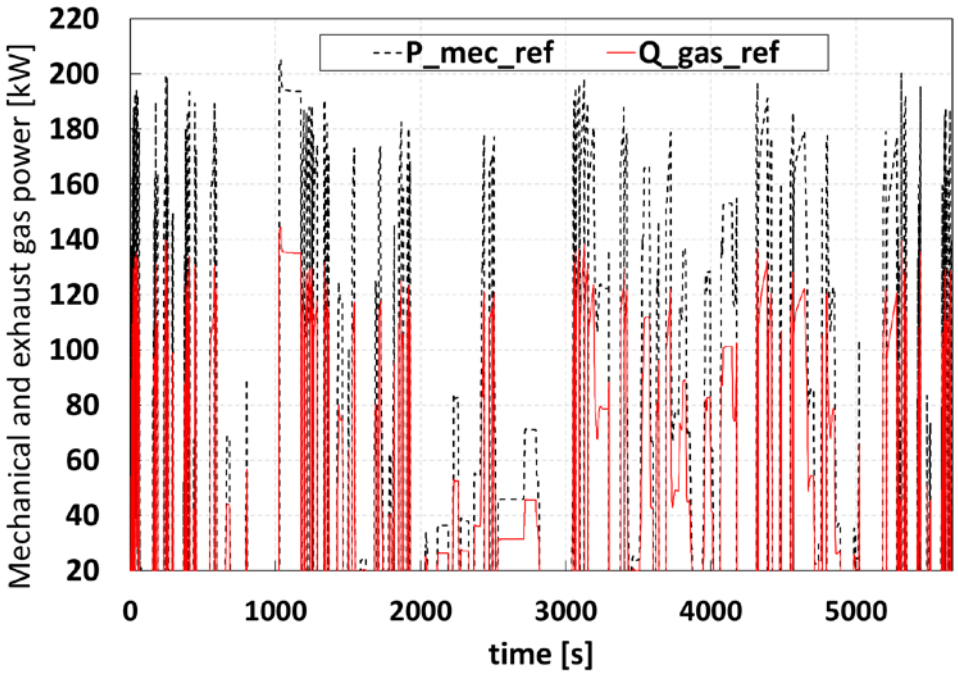

Figure 9. Mechanical power and heat to exhaust gases of the reference engine

According to Figure 9, both terms have similar magnitude order as it was commented in the introduction section when only 30-40% of the available heat is used as mechanical power and almost one third is waste through the exhaust gas system. Thus, there is a potential heat quantity that is waste in CNG engines and its recovery justifies one of the focus of this work.

Figure 10 presents the water temperature at the outlet of the TEG and the radiator of the low temperature cooling circuit for the ACEA cycle. As it can be seen, the temperature of the TEG is kept within the limits stablished by the manufacturer in order to ensure the optimal work of it (20-45ºC). In addition, the correct sizing of the radiator can be observed according to the temperature operation range as it can be seen in the figure.

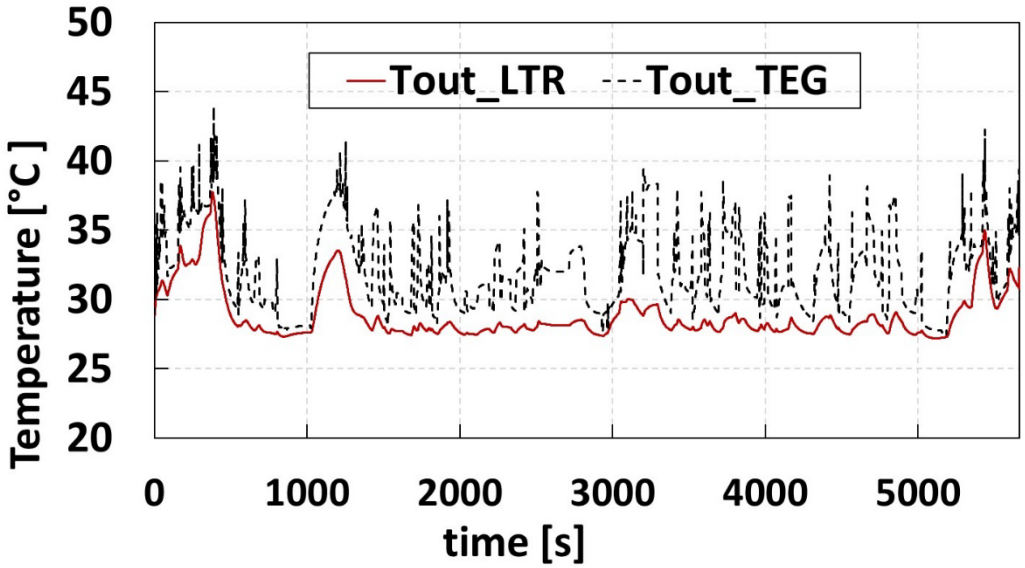

Figure 10. Low temperature radiator and TEG outlet water temperature of the Low Cooling circuit temperature

Figure 11 represents the main temperatures evolution of the high temperature cooling circuit. Initially, the thermostat of this water circuit, is at minimum until the engine temperature reaches the set point (93°C). Afterwards, the flow rate is adjusted based on the instant requirements to ensure the proper cooling of the TBG and the engine being always able to keep the temperature at the outlet of the engine below 100°C set by specifications.

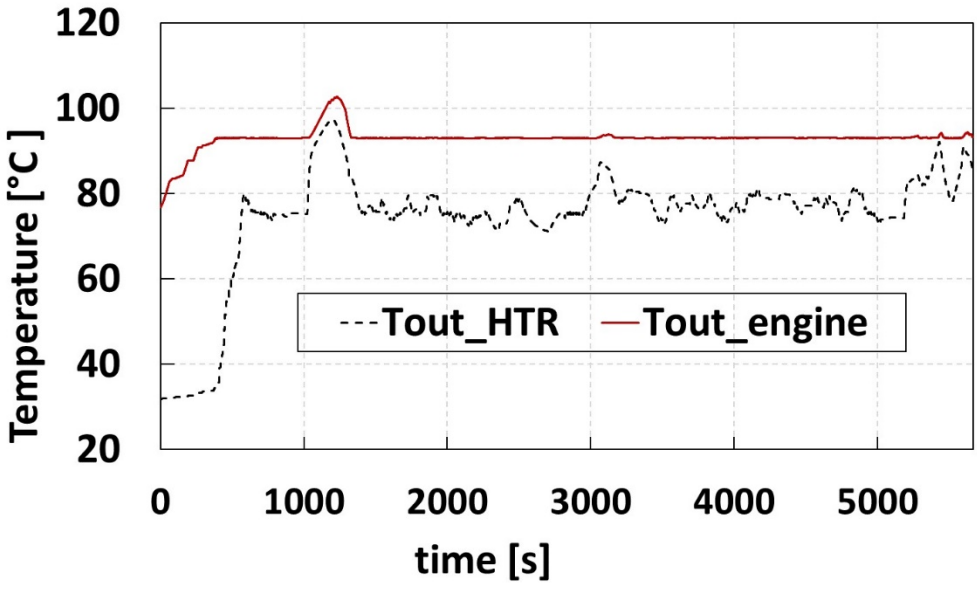

Figure 11. High temperature radiator and engine outlet water temperature of the High temperature Cooling circuit

Figure 12 shows the electric energy consumption of the e-booster for the considered cycle. This element works at low engine speeds and high loads. However, due to the ACEA cycle characteristics, there are only a few points where this component works. Thus, for this application this component has a negligible impact and it is not considered necessary for this type of cycle. See Annex for further explanation.

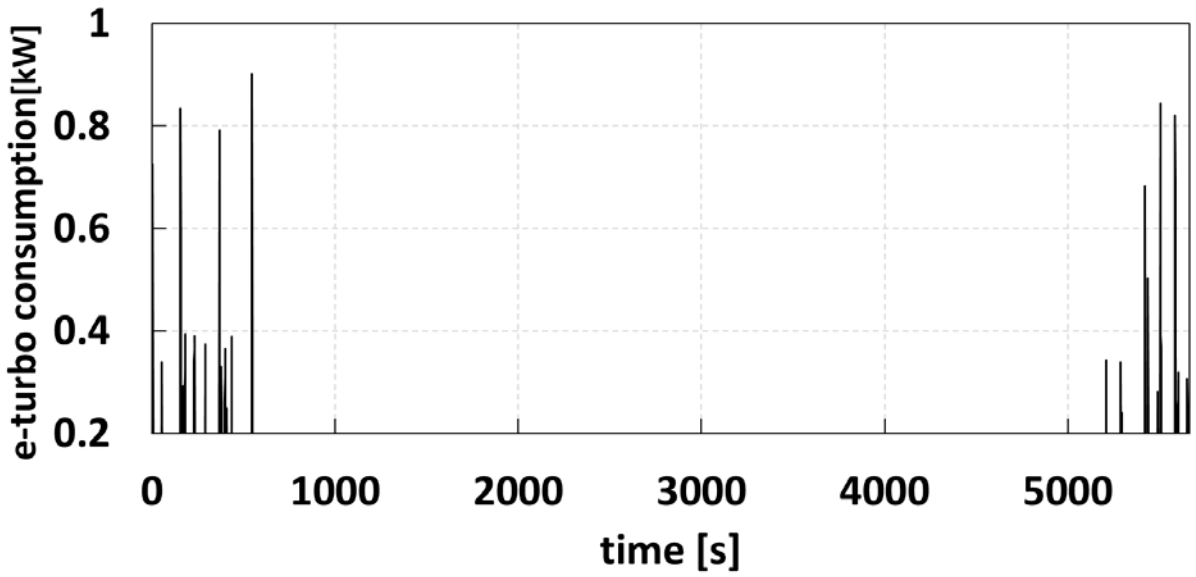

Figure 12. e-booster electric energy consumption

Figure 13 shows the power generated by the TEG. As commented at the beginning of this section, the model has been used in order to find the best configuration of this element according to its characteristics and space constrains. The final configuration consists of 24 cartridges divided in two rows and placed in a circle. This configuration is further explained in the Annex in the part dedicated to this technology.

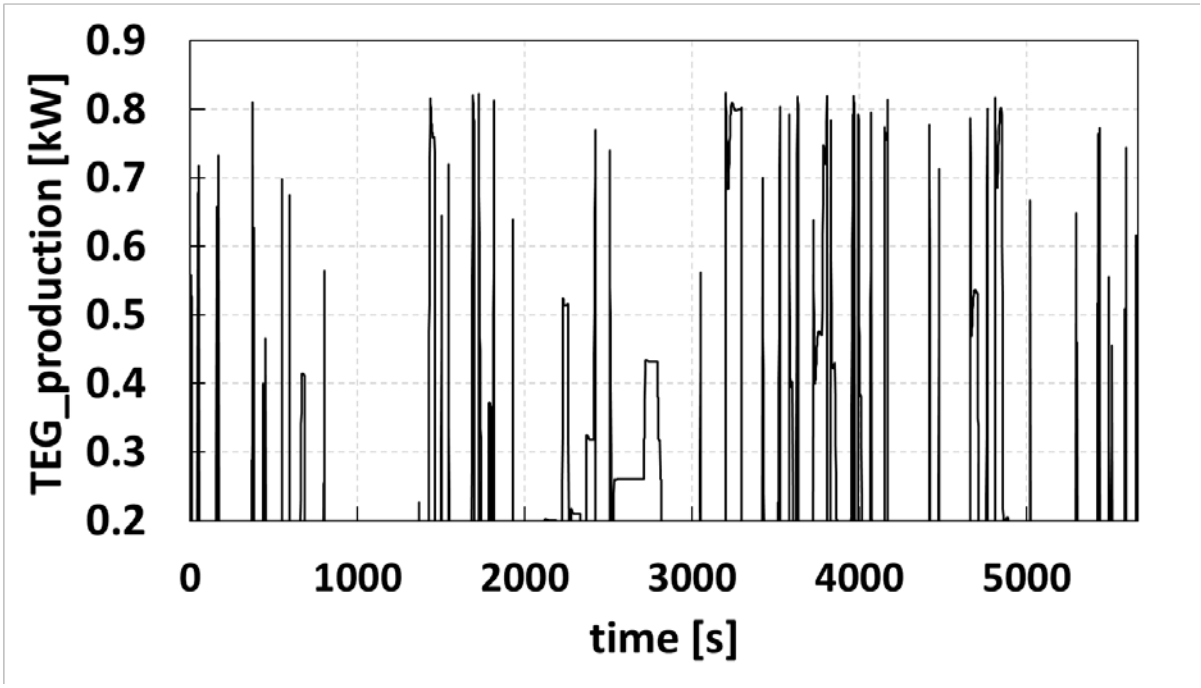

Figure 13. TEG electric production

Following the manufacturer instructions, when the exhaust gas temperature reaches a point that can damage the cartridge or the gas mass flow rate is not sufficient to produce electricity, there is a bypass which deviates all the gas mass flow. Therefore, the TEG does not produce in those periods. The implementation of the proportional bypass controlled only by the maximum temperature would increase significantly the potential of this system. Nevertheless, as a consequence of the temperatures involved and the tolerances allowed, the manufacturer does not recommend that option at this moment.

According to Figure13, the peak electric production is more than 800W. However, based on the bypass conditions imposed by the manufacturer, the TEG is only able to produce in this application about 30% of the total cycle time. From these results it is demonstrated that it is crucial

to address all the technical limitations of the TEG modules in order to be able to have a significant performance of this component which deserves it use in this type of system.

Figure 14 shows the model exhaust gas temperature validation by the representation of the experimental measured TEG inlet temperature and the TEG inlet temperature calculated from the model.

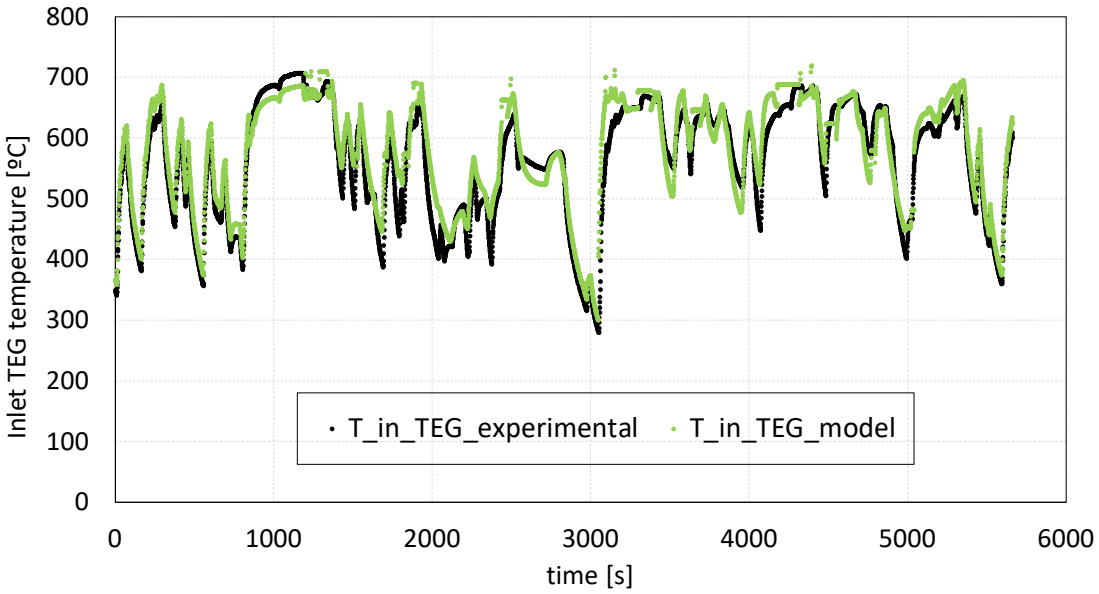

Figure 14: Model and experimental TEG inlet temperature [ºC]

The production of the TBG as a function of the ACEA time can be seen in Figure 15.

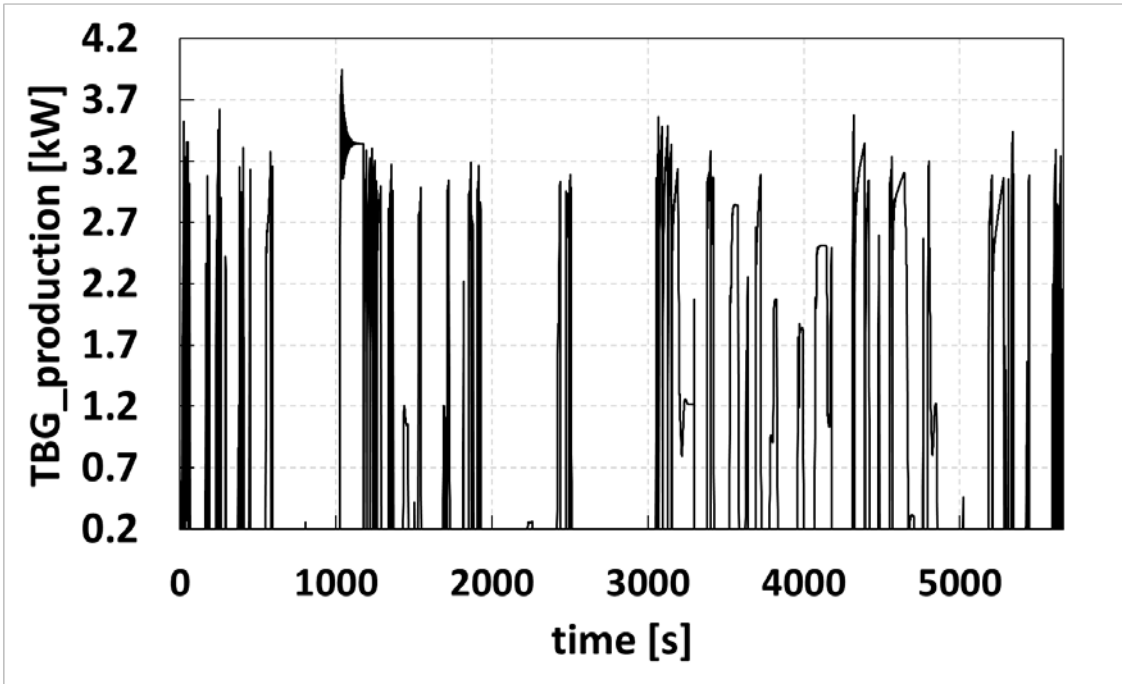

Figure 15. TBG electric production

According to the engine specifications, the maximum allowed back-pressure is 300mbar. Therefore, in order to respect this condition, for this engine and this driving cycle there are periods where the turbine is partially bypassed. In addition, if the gas mass flow is lower than a certain value given by the manufacturer, the turbine is bypassed in order to ensure the component's safety.

In this case, the observed peak electric production reach values up to 3.7kW. Nevertheless, if the backpressure effect would not be considered, this is a potential technology able to produce much more electricity from the exhaust gases.

Figure 16 represents the KERs electric production as a function of time.

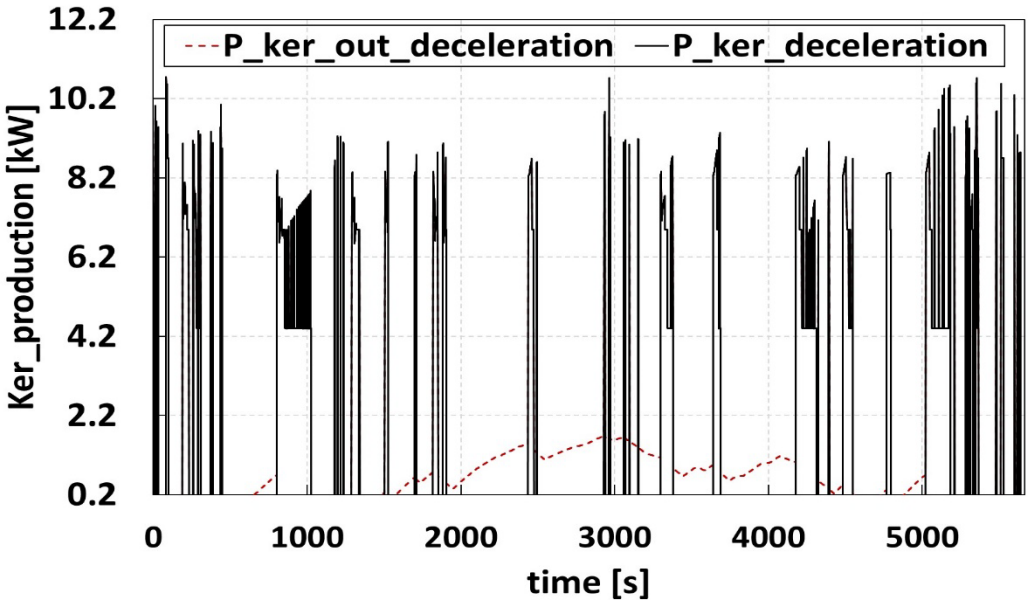

Figure 16. KERs electric production

This technology is the most versatile among the considered technologies. Therefore, the production of the TEG, TBG and the KERs in deceleration periods will be always the maximum possible and, in order to be able to have a net balance equals to zero, the KERs electric production out of deceleration periods is done. The current strategy for KER operation lies on the maximum possible production (limited to 12kW by manufacturer specifications) when there is a deceleration period (free kinetic energy recovery). However, in order to ensure the electric service of the auxiliaries at any time and to have a zero balance at the end of the cycle, the system cannot depend only on the energy recovered from either exhaust gases nor kinetic. Therefore, this system is used also as an energy backup system since the electric production only can be done at any cost by this component.

The model allows the determination of the points where is more suitable from the vehicle efficiency point of view to produce the required extra energy using the KER. The main conclusion of the study resulted, for this KERs, vehicle and mission, in a not considerable influence on the final benefit by producing along different moments. Thus, the final production will be driven by the storage control strategy in order to maintain a zero balance at the end of the mission.

Figure 17 collects the exhaust gas temperature which is released to the ambient for both, the reference and the electrified vehicle. This figure allows the estimation of the lowered temperature after the addition of the TEG and the TBG respectively (the recovered energy).

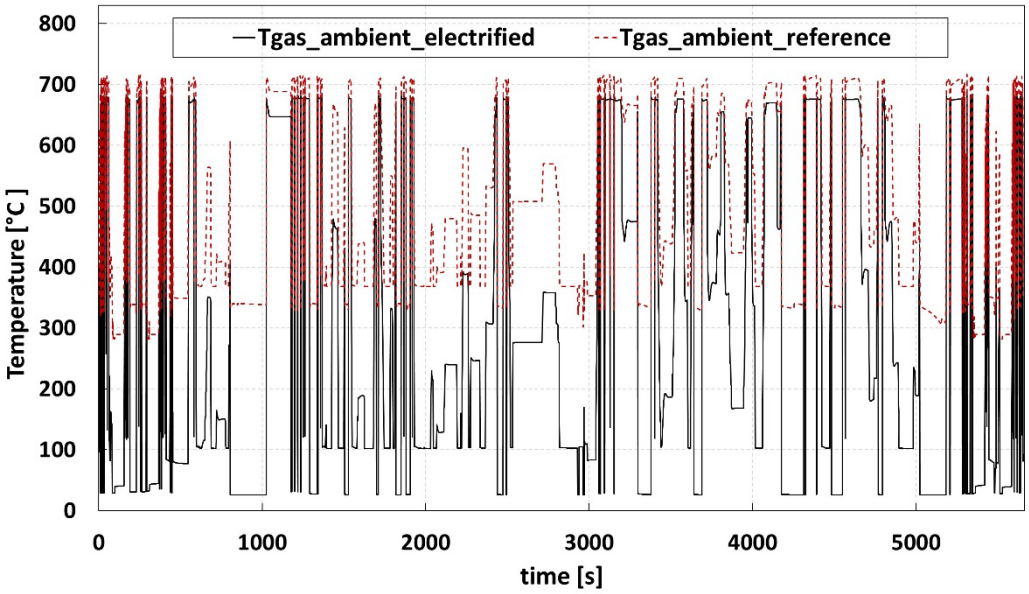

Figure 17. Gas outlet temperature (temperature to the ambient) in the reference vehicle and the electrified vehicle.

Energy inefficiencies as well as the limits of the technologies used to recover the waste energy make impossible to recover 100% of the available heat.

The control strategy of the system is to keep the final level of the battery equals to the initial value so the comparison can be fair. Figure 18 represents the evolution of the state of charge along the ACEA cycle considering all the productions and consumptions.

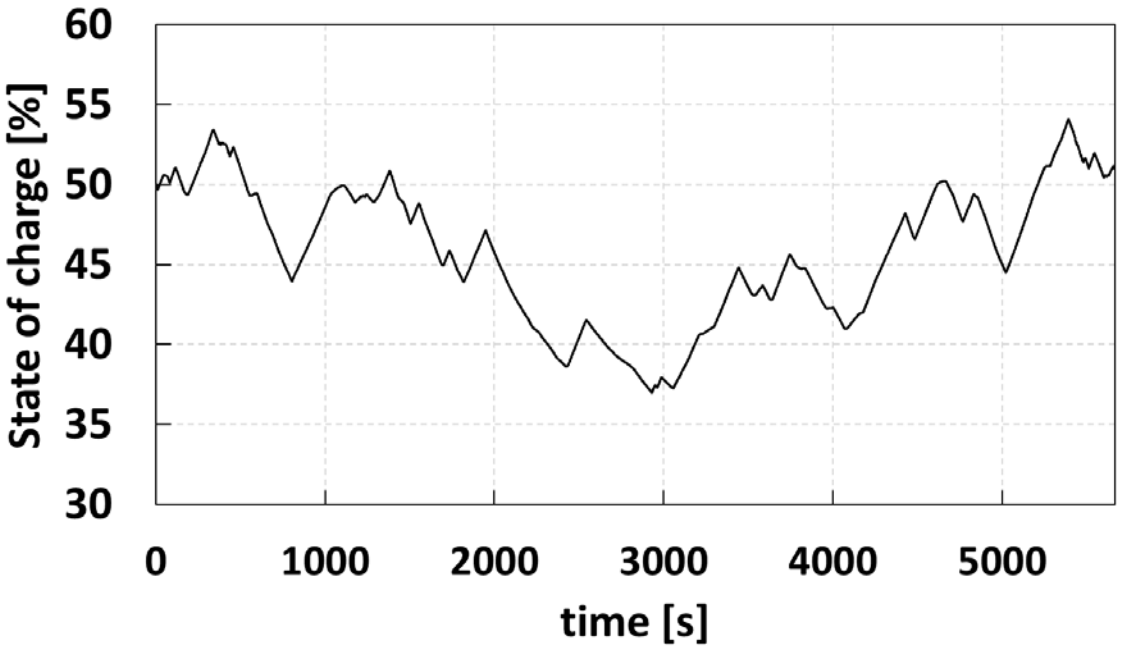

Figure 18. State of the battery charge

At the end of the cycle, the energy balance results in small overproductions. This is due to the followed strategy: in order to maintain the level of the battery at the initial level, the electric production must overcome the losses of the battery and the electric conversion.

The zero balance has been possible by the KERs production out of the deceleration periods. An optimization process to determine the strategy has been done. Table 2 represents some of the cases and the results (expressed in terms of fuel saving) obtained following different KERs production strategies (the DC/DC conversions, battery losses and consumptions are considered in all the cases).

Table 2: Results obtained for different control strategies based on the KERs production

	ACEA CYCLE						
	NONE EXTRA POWER	CONSTANT PRODUCTION	PID 50%	ALL BEGINNING	ALL FINAL	LEVEL < 41.5%	PID 50% from a 3500s
Total production [kWh]	3.607	4.585	4.596	5.203	5.291	4.624	4.633
Total consumption [kWh]	4.366	4.365	4.365	4.364	4.365	4.365	4.365
Balance [kWh]	-0.759	0.22	0.231	0.839	0.926	0.259	0.268
Fuel saved (%)	-	4.703	5.201	4.859	4.848	5.109	4.895

According to the table and the commented in the KERs section, the production of this technology out of deceleration periods does not have a big impact on a vehicle level. Nevertheless, the followed strategy has been to set the PID level of the battery at 50% and adjust it in order to obtain the data expressed in Table 2.

Finally, as it is explained before, the main outcome of the model is the benefit expressed in terms of fuel saving. Figure 19 represents the fuel consumption over the ACEA cycle for both powertrains: the new concept and the reference gas engine vehicle.

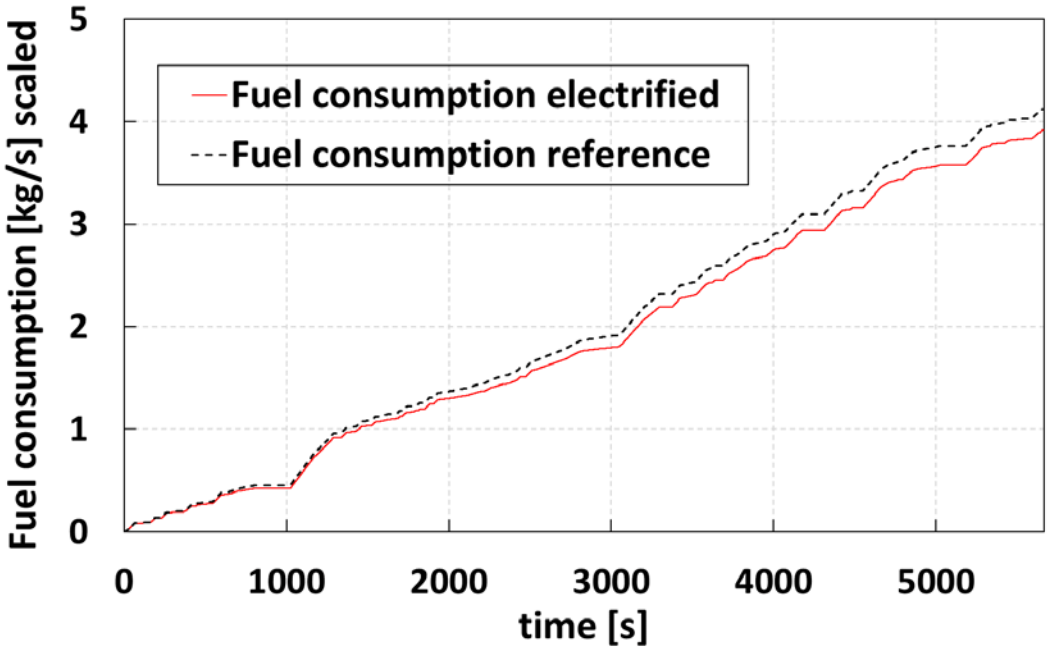

Figure 19. Fuel consumption scaled of the reference vehicle and the electrified vehicle

As it can be observed in this figure, the total fuel saved in this application is up to 5% with a total electric production of 4.5kWh.

Following the same methodology but considering that the vehicle is running at constant speed in the ACEA duration, the same study for the design point (1200 rpm and 600N) can be done. In this case, the fuel saved accounts for a total of 7.5% and 4kWh electric energy production. Table 3 summarizes the main consumptions, productions and the final fuel saved for the ACEA cycle and the vehicles considered in the nominal point.

Table 3. Main results for the design point

	ELECTRIC ENERGY (kWh)
CONSUMED	
Low temp. Water pump	0.4248
High temp. Water pump	1.23
Oil pump	1.447
e-booster	0
Steering pump	0.02292
DCDC	0.1573
Accessories (lighting, …)	1.288
PRODUCED	
TEG	0.81
KERs (deceleration periods)	0
TBG	0.2401
KERs (out of deceleration periods)	3.036
BENEFIT IN TERMS OF FUEL SAVED	
7.5%	

Notice that the KERs production needs to be out of deceleration periods- taking into account its respective consumption penalty- in order to ensure the electric service and zero balance due to the design point considered is a constant value that does not have deceleration periods.

Diesel sensitivity analysis

As a final point, the comparison of the results with a Diesel engine of the same characteristics is presented. The most important differences between the modeled CNG engine and the Diesel engine (both based on experimental data given by the manufacturer) is the exhaust gas mass flow rate (50% higher in Diesel than CNG engines) and the exhaust gas temperature (around 300ºC lower in Diesel engines).

Figure 20 represents the production share (in percentage) by technology for the CNG engine (a) and for the Diesel engine (b) and the ACEA cycle.

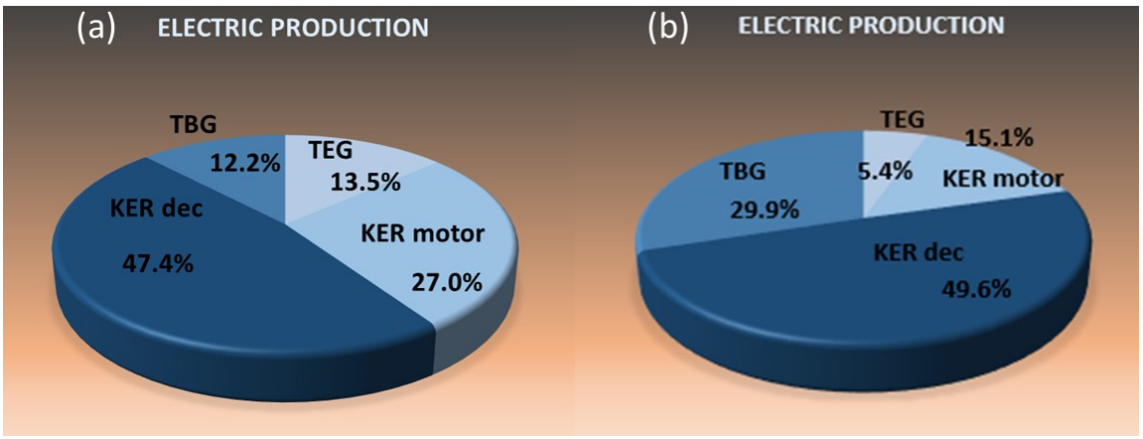

Figure 20: Electric production share by technology for the ACEA cycle. (a) CNG engine (b)DIESEL engine

As it can be seen from the figure, in the Diesel engine the production of the TBG becomes much more important due to the higher gas mass flow employed in this type of engines. Moreover, the electric production of the TEG represents lower percentage in comparison with the CNG engine due to the lower exhaust gas temperatures. The production of the KER system out of deceleration periods (as motor) is lower in Diesel engines thanks to the higher production of the TBG. Therefore, technologies that recuperate energy from temperature are more suitable in CNG engine while technologies that take profit from the gas mass flow are more profitable in Diesel engines.

6. CONCLUSIONS

In current heavy duty vehicles, most of the energy is lost through the exhaust gas system to the ambient. With the available technologies there is not enough potential to efficiently recover it and to have a real impact on the improvement of the vehicle's efficiency. Therefore, the combination and coupling of different technologies is required in order to get the maximum benefit out of it. This challenging work has been analyzed in this work where it is possible to study the contribution of each technology under a vehicle level and for a target driving cycle.

In this paper, the improvement of a vehicle's efficiency by a kinetic energy recovery system, the energy recovery from the exhaust gases by a thermoelectric generator and a turbo-generator, the integration of an e-booster, the modification of the air cooler by a water charge air cooler and the electrification of the main auxiliaries are considered.

Due to the high degree of complexity in such type of problem, a mathematical model was developed. This model has been useful in order to assist on the design phase of the components as well as on the development of optimal control strategies by the anticipation of the influence of any parameter change in order to maximize the reduction of the fuel consumption.

The developed models for the different subsystems have been validated individually and the obtained mean errors are lower than 5% for all the modules.

From the results obtained with the model, the following conclusions based on the contribution of each technology for the ACEA driving cycle are extracted:

- WCAC: In the studied case, with the available specifications of the engine's performance given by the manufacturer, the control of the variables at the inlet of the manifold does not have a significant influence on the final fuel saved for this mission, engine and vehicle.
- E-booster: an exhaustive study of the application of this component and its strategy has been done. However, for the chosen mission, vehicle and engine, its use does not reflect an influence on the vehicle efficiency. Nevertheless, and based on the influence of this device on the engine map, it would become much more important in another kind of application such as urban cycles or different vehicles (i.e. buses).
- KERs: this technology has a great potential due to, mainly, its versatility and its kinetic energy recovery efficiency. On the one hand, the maximum energy available to recover during deceleration periods (braking energy) is "freely" done with a high level of efficiency. Thus, accounting for important electric production. On the other hand, in order to have a zero balance at the end of a cycle, more electric energy is required in this cycle and has been produced with the KERs out of the deceleration periods. A deep study in order to determine the most convenient periods to produce out of deceleration (considering a torque penalty) was carried out even though not a considerable influence has been obtained. As a result, in this type of cycles as well as for the considered vehicle,

this device represents a very important component that allows a big rise on the efficiency if its operation is implemented properly.

- TEG: The optimization of its design has allowed the maximization of the final electric production. However, and in spite of the initial potential of this technology derived from the high exhaust gases temperature, the temperature limitations of the materials have constrained significantly the initial potential of this technology. Nevertheless, the use of this type of technology is much profitable in CNG engines than in Diesel engines.
- TBG: The increase of the backpressure is a penalty that limits the potential of this component. In fact, for the considered engine and turbine, there are several periods where it has to be bypassed in order to do not overcome the maximum allowed backpressure. Nevertheless, based on the results extracted from the model not considering the backpressure bypass, this technology shows a very important potential on the electric production, much more interesting in Diesel engines due to its higher exhaust gas mas flow.
- Storage level: the level of the battery is a crucial parameter that must ensure the proper electric feeding of the auxiliaries at any moment. In this sense, mathematical models play an important role and have helped to find the solution that maximizes the saving by the possibility of simulate a complete cycle as it has been presented in the results section for this application.

As an example, a design point has been considered applying a constant engine speed and torque with the same duration as the ACEA cycle (1200 rpm and 600N) accounting for an electric energy production up to 4kWh and a fuel saving of 7,5%.

Acknowledgements

This work has been developed in the frame of the project of the European Seventh Union Framework Program by the project High efficiency energy conversion for future heavy duty transport High efficiency energy conversion for future heavy duty transport GASTone grant agreement 605456. The authors are grateful for the given support.

References

[1] U.S Energy Information Administration. International Energy Outlook 2016. vol. 484. 2016.

[2] European Union. Regulation (EC) No. 443/2009 – setting emission performance standards for new passenger cars as part of the Community's integrated approach to reduce CO2 emissions from light-duty vehicles. Off J Eur Union 2014.

[3] Di Battista D, Mauriello M, Cipollone R. Waste heat recovery of an ORC-based power unit in a turbocharged diesel engine propelling a light duty vehicle. Appl Energy 2015;152:109–20. doi:10.1016/j.apenergy.2015.04.088.

[4] Morgan R, Dong G, Panesar A, Heikal M. A comparative study between a Rankine cycle and a novel intra-cycle based waste heat recovery concepts applied to an internal combustion engine. Appl Energy 2016;174:108–17. doi:10.1016/j.apenergy.2016.04.026.

[5] Xie H, Yang C. Dynamic behavior of Rankine cycle system for waste heat recovery of heavy duty diesel engines under driving cycle. Appl Energy 2013;112:130–41. doi:10.1016/j.apenergy.2013.05.071.

[6] GASTONE Project FP7-Transport, FP7-SST-2013-RTD-1, Grant Agreement no 605456 n.d. http://gastone-project.webs.upv.es/.

[7] Fu J, Liu J, Feng R, Yang Y, Wang L, Wang Y. Energy and exergy analysis on gasoline engine based on mapping characteristics experiment. Appl Energy 2013;102:622–30. doi:10.1016/j.apenergy.2012.08.013.

[8] Shabashevich A, Richards N, Hwang J, Erickson PA. Analysis of powertrain design on effective waste heat recovery from conventional and hybrid electric vehicles. Appl Energy 2015;157:754–61. doi:10.1016/j.apenergy.2015.02.067.

[9] Birkholz, U. et al. Conversion of Waste Exhaust Heat in Automobile using FeSi2 thermoelements. Proc. 7th Int. Conf. Thermoelectr. Energy Convers., n.d., p. 124–128.

[10] Karri MA, Thacher EF, Helenbrook BT. Exhaust energy conversion by thermoelectric generator: Two case studies. Energy Convers Manag 2011;52:1596–611. doi:10.1016/j.enconman.2010.10.013.

[11] Saidur R, Rezaei M, Muzammil WK, Hassan MH, Paria S, Hasanuzzaman M. Technologies to recover exhaust heat from internal combustion engines. Renew Sustain Energy Rev 2012;16:5649–59. doi:10.1016/j.rser.2012.05.018.

[12] Capata R, Toro C. Feasibility analysis of a small-scale ORC energy recovery system for vehicular application. Energy Convers Manag 2014;86:1078–90. doi:10.1016/j.enconman.2014.06.024.

[13] Galindo J, Ruiz S, Dolz V, Royo-Pascual L, Haller R, Nicolas B, et al. Experimental and thermodynamic analysis of a bottoming Organic Rankine Cycle (ORC) of gasoline engine using swash-plate expander. Energy Convers Manag 2015;103:519–32.

598 doi:10.1016/j.enconman.2015.06.085.

599 [14] Horst TA, Rottengruber H-S, Seifert M, Ringler J. Dynamic heat exchanger model for
600 performance prediction and control system design of automotive waste heat recovery
601 systems. Appl Energy 2013;105:293–303. doi:10.1016/j.apenergy.2012.12.060.

602 [15] Feru E, Willems F, de Jager B, Steinbuch M. Modeling and Control of a Parallel Waste
603 Heat Recovery System for Euro-VI Heavy-Duty Diesel Engines. Energies 2014;7:6571–92.
604 doi:10.3390/en7106571.

605 [16] Murgovski N, Marinkov S, Hilgersom D, De Jager B, Steinbuch M, Sjöberg J.
606 ScienceDirect Powertrain sizing of electrically supercharged internal combustion engine
607 vehicles. IFAC-PapersOnLine 2015;48:101–8. doi:10.1016/j.ifacol.2015.10.015.

608 [17] Arsie I, Cricchio A, Pianese C, Cesare M De, Nesci W, Marelli M, et al. A Comprehensive
609 Powertrain Model to Evaluate the Benefits of Electric Turbo Compound (ETC) in
610 Reducing CO2 Emissions from Small Diesel Passenger Cars. SAE Tech Pap 2014.
611 doi:10.4271/2014-01-1650.Copyright.

612 [18] Hsiao YY, Chang WC, Chen SL. A mathematic model of thermoelectric module with
613 applications on waste heat recovery from automobile engine. Energy 2010;35:1447–54.
614 doi:10.1016/j.energy.2009.11.030.

615 [19] Deng YD, Hu T, Su CQ, Yuan XH. Fuel Economy Improvement by Utilizing Thermoelectric
616 Generator in Heavy-Duty Vehicle. J Electron Mater 2016:1–8. doi:10.1007/s11664-016-
617 4996-1.

618 [20] Högblom O, Andersson R. A simulation framework for prediction of thermoelectric
619 generator system performance. Appl Energy 2016;180:472–82.
620 doi:10.1016/j.apenergy.2016.08.019.

621 [21] Crane D, Lagrandeur J, Jovovic V, Ranalli M, Adldinger M, Poliquin E, et al. TEG on-
622 vehicle performance and model validation and what it means for further teg
623 development. J Electron Mater 2013;42:1582–91. doi:10.1007/s11664-012-2327-8.

624 [22] Patterson ATC, Tett RJ, McGuire J. Exhaust Heat Recovery using Electro-
625 Turbogenerators, 2009. doi:10.4271/2009-01-1604.

626 [23] Mamikoglu S, Andric J, Dahlander P. Impact of Conventional and Electrified Powertrains
627 on Fuel Economy in Various Driving Cycles, 2017. doi:10.4271/2017-01-0903.

628 [24] Pasunurthi S, Jupudi R, Wijeyakulasuriya S, Gubba SR, Im H, Mubarak Ali MJ, et al. Cycle
629 to Cycle Variation Study in a Dual Fuel Operated Engine, 2017. doi:10.4271/2017-01-
630 0772.

631 [25] Mahmoud M, Garnett R, Ferguson M, Kanaroglou P. Electric buses: A review of
632 alternative powertrains. Renew Sustain Energy Rev 2016;62:673–84.
633 doi:10.1016/j.rser.2016.05.019.

634 [26] Laboe K, Canova M. Powertrain Waste Heat Recovery: A Systems Approach to Maximize
635 Drivetrain Efficiency. ASME 2012 Intern. Combust. Engine Div. Spring Tech. Conf.,
636 ASME; 2012, p. 985. doi:10.1115/ICES2012-81160.

637 [27] Feru E, Kupper F, Rojer C, Seykens X, Scappin F, Willems F, et al. Experimental
638 Validation of a Dynamic Waste Heat Recovery System Model for Control Purposes,
639 2013. doi:10.4271/2013-01-1647.

640 [28] LaGrandeur J, Crane D, Hung S, Mazar B, Eder A. Automotive Waste Heat Conversion to

Electric Power using Skutterudite, TAGS, PbTe and BiTe. 2006 25th Int. Conf. Thermoelectr., IEEE; 2006, p. 343–8. doi:10.1109/ICT.2006.331220.

[29] Hasewend W. AVL Cruise — Driving performance and fuel consumption simulation. ATZ Worldw 2001;103:10–3. doi:10.1007/BF03226780.

[30] Saidur R, Rezaei M, Muzammil WK, Hassan MH, Paria S, Hasanuzzaman M. Technologies to recover exhaust heat from internal combustion engines. Renew Sustain Energy Rev 2012;16:5649–59. doi:10.1016/j.rser.2012.05.018.

[31] The Mathworks Inc., MATLAB & Simulink R2009b, Computer Software, Natick, Massachusetts, USA 2009. Matlab/Simulink n.d.

[32] Energy. USD of, LLC UcA. Autonomie 2014.

[33] 2015 ACEA. Ave Des Nerviens 85, B-1040 Brussels, Belgium 2015. http://www.acea.be/.

[34] Saidur R, Rezaei M, Muzammil WK, Hassan MH, Paria S, Hasanuzzaman M. Technologies to recover exhaust heat from internal combustion engines. Renew Sustain Energy Rev 2012;16:5649–59. doi:10.1016/j.rser.2012.05.018.

[35] Bass, John C. (Hi-Z Technology I), Campana RJ, Elsner NB. Thermoelectric Generator Development for Heavy-Duty Truck Applications. SAE Publ 1992:743–50.

[36] Cibulka J. KINETIC ENERGY RECOVERY SYSTEM BY MEANS OF FLYWHEEL ENERGY STORAGE. Adv Eng 2009;31:1846–5900.

LIST OF FIGURES

ANNEX

The model equations as well as a further explanation of the followed methodology is summarized in this annex.

Block 1: CNG gas engine

The Mechanical power is obtained directly from the inputs based on the general expression shown in Eq.1:

$$P[W] = \frac{2\pi}{60} \cdot n \cdot Torque \tag{1}$$

The air mass flow rate [kg/s] is calculated according to the Eq.2

$$ma[kgs^{-1}] = mf \cdot \lambda \cdot AFR_{stec} \tag{2}$$

Where the fuel consumption is calculated from a correlation function of the engine torque and speed.

Figure 1 represents the engine normalized fuel consumption correlated and experimental (a) function of the engine torque and (b) function of the engine speed.

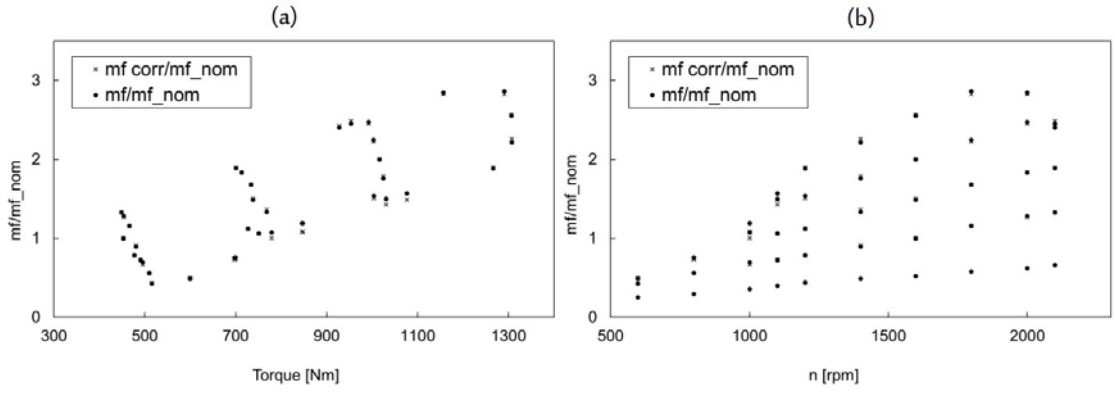

Figure 1: Normalized fuel consumption engine validation. (a) with the engine torque and (b) the engine speed

The heat loss to exhaust gases and to the ambient is calculated from a correlation function of the engine power and based on experimental data.

The heat dissipated by the radiator of the high temperature cooling circuit is directly calculated from the balance shown in Eq. 3.

$$Q_{rad}[W] = Q_f - P - Q_{gas} - Q_{amb} \quad (3)$$

The water mass flow rate from of the high temperature cooling circuit was obtained from a fitting function of the engine speed.

The heat removed by the Air Cooler, $Q_{AC}[W]$ as well as the exhaust gas temperature (T_7) are based on correlations from experimental data.

All the data explained above represents the characteristics of the reference vehicle. However, in order to predict the behavior of the new concept vehicle, it is necessary to consider the drawback of the addition of the new energy recovery systems downstream of the manifold since they will increase the back-pressure. To evaluate the back-pressure effect on the torque request, a correction of it has been applied based on the Eq. 4.

$$\Delta\tau_{\Delta press} = \tau_e^{'} - \tau_e = \tau_e \cdot \frac{\Delta P_e}{bmpe} = \frac{\Delta P_e \cdot V_d}{4\pi} \quad (4)$$

Block 2: High temperature cooling circuit

- **Radiators**

The same methodology based on general energy balance equations according to the Eq. 5 for their modelling has been followed for both radiators.

$$C \cdot \frac{dT_{out}}{dt} = \dot{m}_w \cdot cp_w \cdot (T_{in\_rad} - T_{out\_rad}) - \varepsilon \cdot \dot{m}_{a\_vehi} \cdot cp_a \cdot (T_{outa\_rad} - T_{ina\_rad}) \quad (5)$$

Where C [JK^{-1}] is the thermal capacity of each radiator and cp [$Jkg^{-1}K^{-1}$] is the specific heat of the correspondent fluids given as an input of the model. While ε is the effectiveness and is calculated in another subsystem based on the NTU Relationships for two-stream Heat Exchangers [24] as it is expressed in Eq. [6-10].

$$\varepsilon = \frac{Q}{C_{\min} \cdot (T_{ina\_rad} - T_{in\_rad})} \quad (6)$$

$$\varepsilon = 1 - e^{\left[\frac{NTU^{0.22}(\cdot e^{[-C^* \cdot NTU^{0.78}]} - 1)}{C^*}\right]} \quad (7)$$

$$NTU = \frac{UA}{cp_a \cdot \dot{m}_{a\_vehi}} \quad (8)$$

$$C^* = \frac{C_{\min}}{C_{\max}} = \frac{cp_a \cdot \dot{m}_{a\_vehi}}{cp_w \cdot \dot{m}_w} \quad (9)$$

$$UA = \frac{1}{\frac{1}{h_i \cdot A_i} + \frac{1}{h_e \cdot (A_w + \eta A_f)}} \quad (10)$$

For the UA expression in Eq. 10 an accurate fitting function of the water and the air mass flow rate has been found and predicts the behavior with a high level of confidence for both radiators and the WCAC. It is expressed in the Eq.11.

$$UA = \frac{1}{\frac{1}{K_1 \cdot \dot{m}_a^{n1}} + \frac{1}{K_2 \cdot \dot{m}_w^{n2}}} \quad (11)$$

Where K_1, K_2, n_1 and n_2 are constants adjusted respectively for each radiator and the WCAC based on experimental data given from each component. Therefore, these constants are required inputs of the model.

The last element considered in this block is the engine. A dynamic energy balance is implemented (Eq. 12) to model its temperature and, therefore, being able to maintain it at the set point given as an input.

$$C_{eng} \cdot \frac{dT_{eng}}{dt} = \dot{Q}_{rad} - \dot{m}_{w,HTR} \cdot cp_w \cdot (T_{wout,eng} - T_{win,eng}) \quad (12)$$

Where Q_{rad} [W] is the heat dissipated by the radiator and the outlet engine temperature is the set point fixed in 93ºC.

Block 3: Low temperature cooling circuit

The same methodology as it has been detailed above is used.

Block 4: Water pumps and Block 5: Electrified auxiliaries

Block 6: High temperature water pump

The modelling of the mechanical and the electric high temperature water pump have been integrated into the model. The required pressure by the pump is calculated considering the engine drop pressure, the radiator drop pressure and the circuit losses. The models of the drop pressures are based on fittings from experimental data accurate enough as their validation show for example for the radiator in Figure 2.

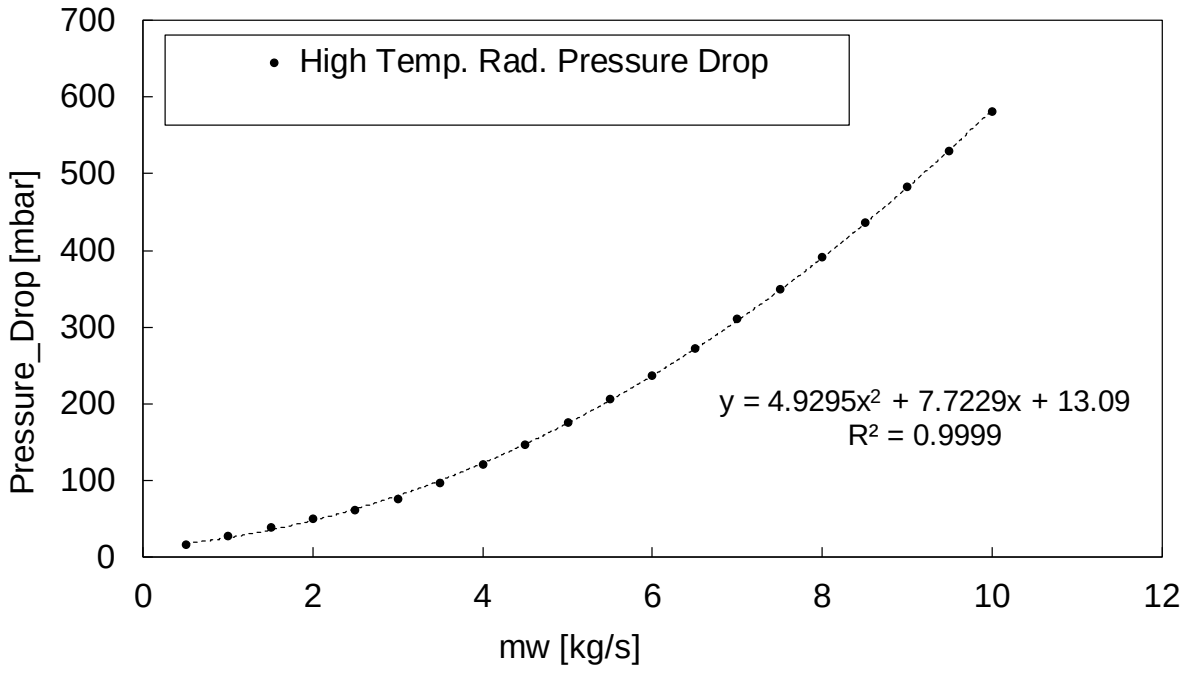

Figure 2. Water high temp. Radiator drop pressure fitting

The two pumps and has been modelled based on experimental data from the current and the electric manufacturer pump. The hydraulic power is calculated from a correlation function of the pressure, the engine speed and the water mass flow rate. Then, the mechanical power is directly calculated by considering the efficiency function of the engine speed.

Regarding to the electric pump, the pump speed is calculated thanks to a surface fitting function of the water mass flow rate (given as an input) and the required pressure (calculated as it was explained above). With the pump speed and the water mass flow rate, another surface fitting is used to calculate the electric power consumption [W].

Finally, in the low temperature water loop system, the same approach for the calculation of the required pressure has been followed. The water drop pressure through all the components in the low temperature water loop (low temperature radiator, WCAC, KER, TEG) as well as the model of the electrical pump are based on correlations validated with experimental data that account with an error lower than 1%.

Block 7: e-booster

To consider the influence of this component on the efficiency, the maximum load of the engine an extension of the engine's characteristic curve for low engine speed (the main use of this element) was developed based on correlations from experimental data of the engine given by the manufacturer.

Figure 3 represents the specific fuel consumption normalized for the engine including the new area defined (pattern black line area).

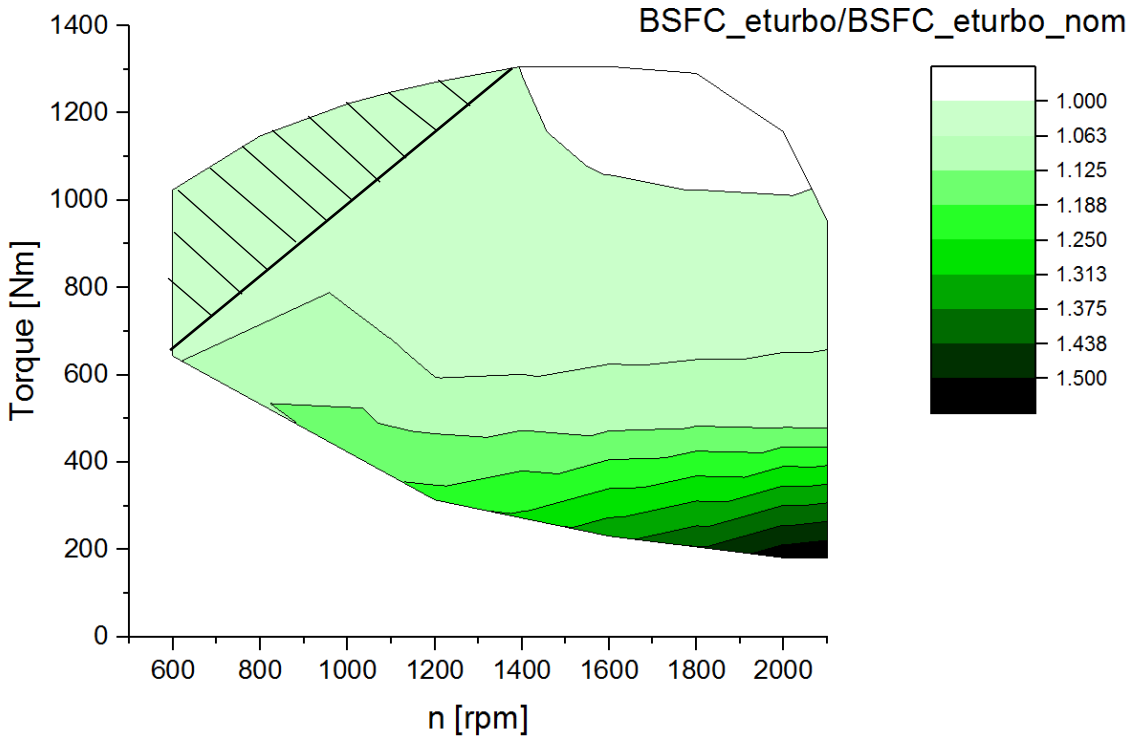

Figure 3: Specific fuel consumption/Nominal Specific fuel consumption including the e-turbo

The correction of the new fuel consumption has been made based on the assumption of a constant temperature so the density function of the pressure according to Eq.13-15.

Eq.13 and Eq.14 represent the air mass flow rate to the manifold for the reference's vehicle (ma) and the electrified vehicle (ma').

$$ma = \eta_v \cdot \rho \cdot V_d \cdot \frac{n}{2} = \eta_v \cdot \rho(T, \Pr ess) \cdot V_d \cdot \frac{n}{2} = \eta_v \cdot \rho(\Pr ess) \cdot V_d \cdot \frac{n}{2} \quad (13)$$

$$ma' = \eta_v \cdot \rho' \cdot V_d \cdot \frac{n}{2} = \eta_v \cdot \rho'(T, \Pr ess) \cdot V_d \cdot \frac{n}{2} = \eta_v \cdot \rho'(\Pr ess) \cdot V_d \cdot \frac{n}{2} \quad (14)$$

Assuming that the air density is function only of the pressure and constant temperature, Eq.15 is obtained

$$\frac{ma'}{ma} = \frac{\rho'}{\rho} = \frac{P'}{P} = \Pr \quad (15)$$

Applying then a linear fitting from the full load's curve of the reference vehicle, the pressure is correlated function of the engine speed so the new air mass flow rate for the full load's curve is obtained.

The fuel mass flow rate is given by the stoichiometric relation from the air mass flow rate as previously done in the engine's block.

The model of the e-turbo is given by the manufacturer and integrated into the model system with a high level of accuracy according to Figure 4 and Figure 5.

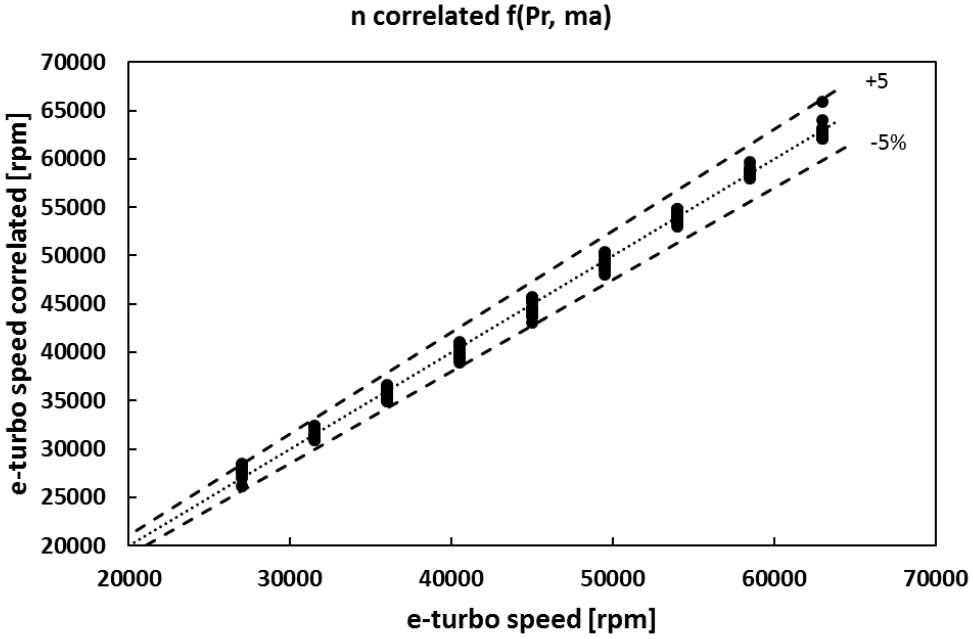

Figure 4. e_turbo speed correlation error

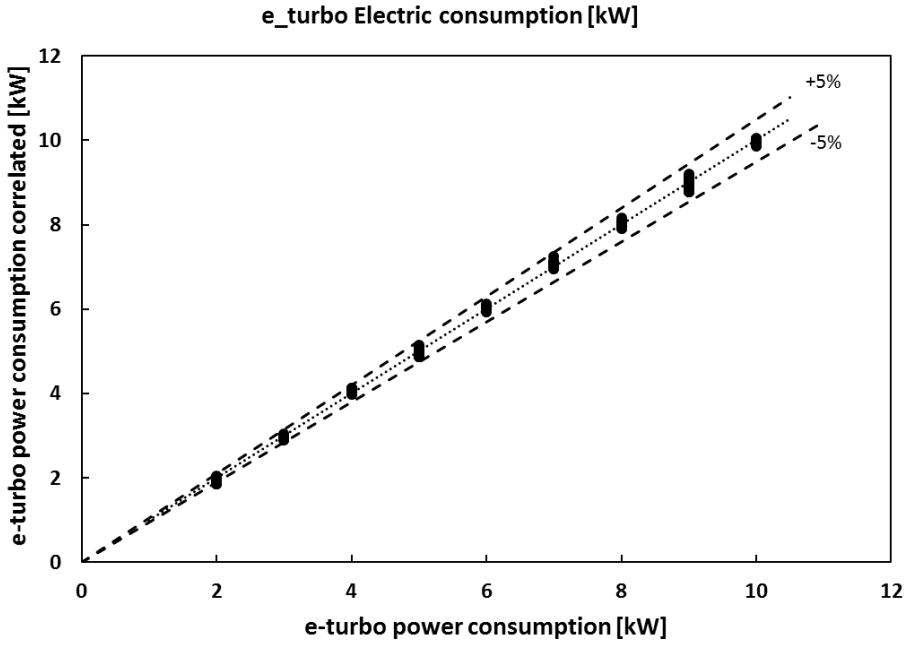

Figure 5. e_turbo power consumption fitting accuracy

Block 8: Thermo Electric Generator

The methodology followed for its modelling is based on correlations from experimental data and basic heat transfer equations. In order to obtain the electrical power output, it is assumed that the power produced will be much lower than the heat transfer between the hot and the cold side. First, in Figure 6 a correlation with high level of confidence (R2=0.9988) between the power and the exhaust gases heat from experimental data has been employed. Data is normalized to be shown on the graph.

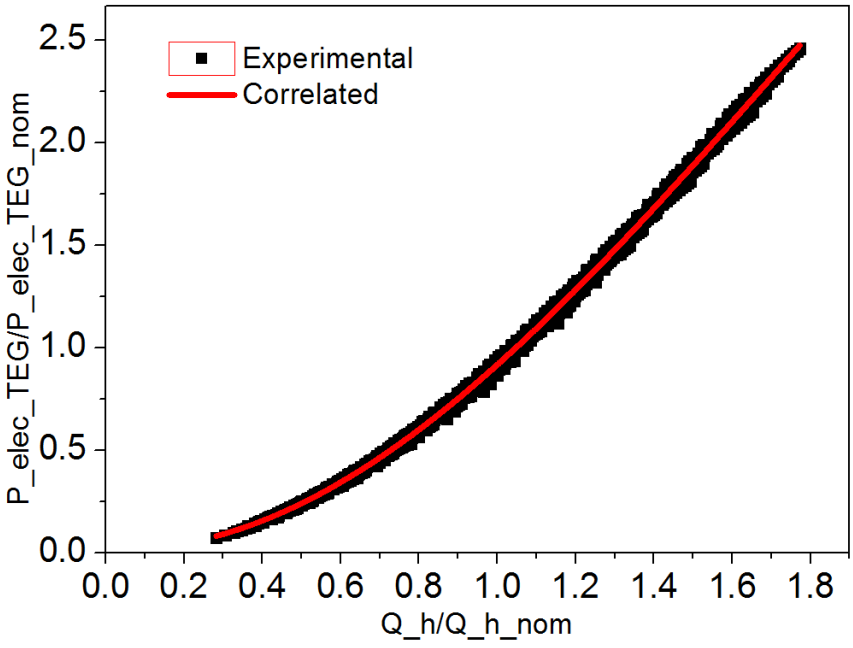

Figure 6. Pelec TEG [W] vs Q_gas [kW] fitting validation.

Second, the gas outlet temperature is obtained from the basic heat transfer equation. Eq. 16.

$$Q_h(kW) = Q_{gas} = m_g \cdot (T_{gin} - T_{gout}) \quad (16)$$

Where the exchanged heat from the TEG module is calculated following the Eq. 17.

$$Q_{gas}(W) = \varepsilon_{TEG} mcp_{\min} \cdot (T_{gin} - T_{win}) \quad (17)$$

808 And the effectiveness has been calculated as in the radiators following the expressions for cross
809 flow heat exchangers. Eqs.7-9.

810 And the UA values have been estimated from experimental data and a surface fitting function of
811 the gas mass flow rate and the average water and gas temperatures has been used.

812 $$UA = b \cdot m_g^x + c \cdot T_g + d \cdot T_w \quad (18)$$

813 Where x,b,c and d are constants estimated for the TEG considered in the project.

814 Finally, the outlets temperatures are directly calculated from the heat transfer equations given in
815 Eq. 19 and Eq. 20.

816 $$T_{wout} = \frac{Q_{gas}}{mCp_w} + T_{win} \quad (19)$$

817 $$T_{gout} = T_{gin} - \frac{Q_{gas}}{mCp_g} \quad (20)$$

818 Obtaining a pretty good results based on the validation with experimental data as it can be seen
819 in the Figure 7 for example for the gas outlet temperature.

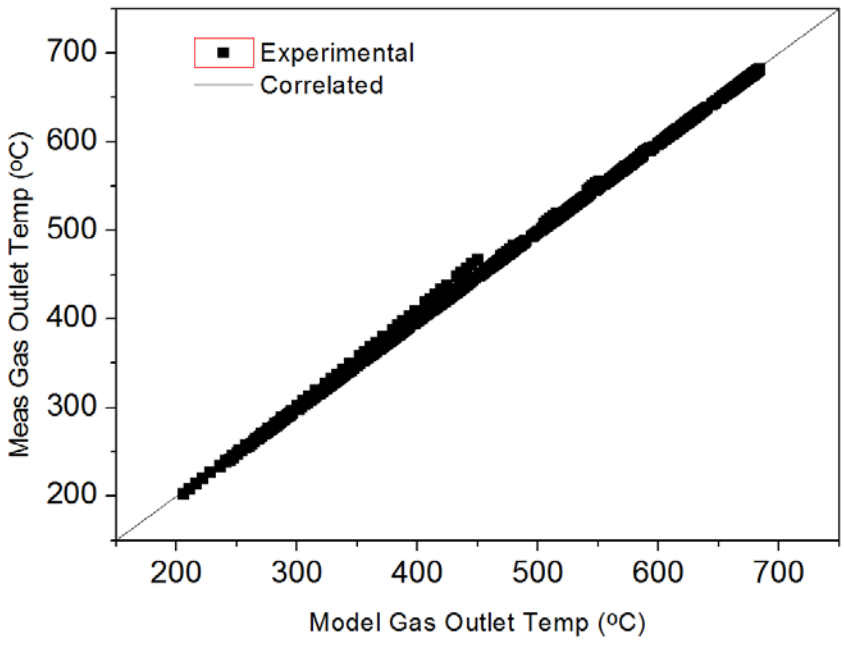

820

821 Figure 7. TEG Exhaust gas outlet temperature fitting validation.

822 The final outlet temperature is calculated from the mixed between the by-pass and gas outlet
823 temperature.

824 Furthermore, the results from the previous equations are only for one cartridge. Nevertheless, the
825 number of cartridges, their arrangement as well as the definition of the optimal sizing for this
826 application needs to be done.

827 The final configuration consists of a combination of 24 cartridges divided in two rows with the
828 two passes cooling circuit in order to ensure a proper temperature difference while maintaining
829 the safety of the cartridges. In addition, the incorporation of the required by-pass to avoid the
830 damage of the cartridges because of an excessive temperature or not enough exhaust gas mass
831 flow is able to gradually open and close so the maximum production is always ensured.

832 Figure 8 shows the experimental and the model electric production prediction based on the
833 conditions specified in Table 1.

834 Table 1. Experimental conditions of the TEG measures

Variable	**Measurement**
mw/cartridge [lpm]	2
Twater_inlet [ºC]	15-35
Gas mass flow rate [kg/h]	150-300
Inlet gas temperature [ºC]	200-500

835

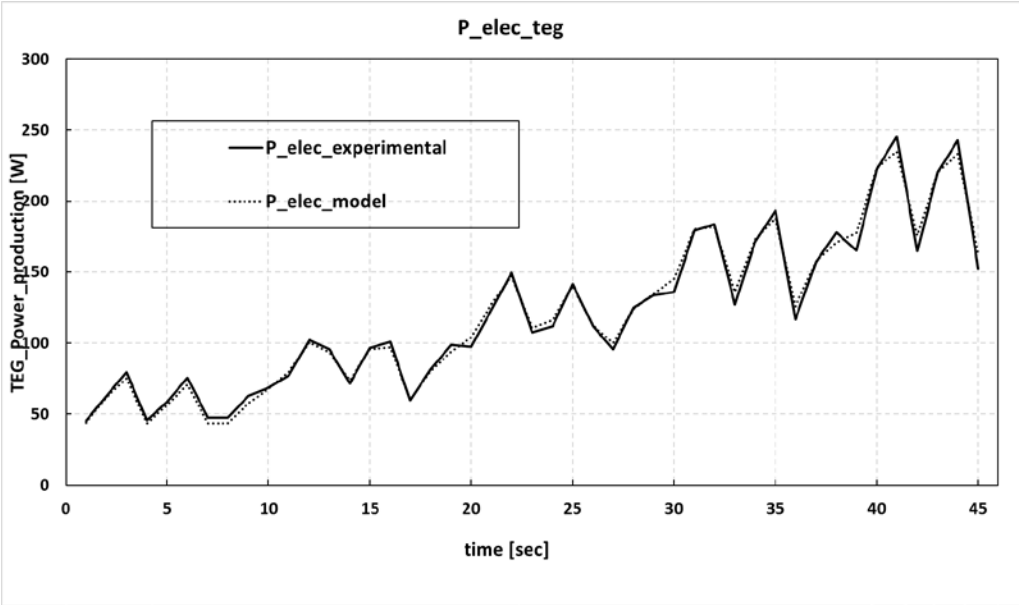

Figure 8. TEG model validation

Finally, the global results for this application, are calculated in Eqs.[21-24]:

$$P_{total\_elec} = n_{cartrg/row1} \cdot P_{elec1} + n_{cartrg/row2} \cdot P_{elec2} \quad (21)$$

$$m_{total\_water} = n_{cartrg/row} \cdot m_{w,cartg} \quad (22)$$

$$T_{w\_out} = \frac{Q_2}{mcpw} + T_{w\_in2} = \frac{Q_2}{mcpw} + \frac{Q_1}{mcpw} + T_{w\_in1} \quad (23)$$

$$T_{g\_out} = T_{g\_in2} - \frac{Q_2}{m_{g2}cp_g} = \begin{array}{l} ([(T_{g\_in1} - \frac{Q_1}{m_{g1}cp_g}) \cdot \beta_{TEG} + (1-\beta_{TEG}) \cdot T_{g\_in1}] - \frac{Q_2}{m_{g2}cp_g}) \cdot \lambda_{TEG} + \\ + [(T_{g\_in1} - \frac{Q_1}{m_{g1}cp_g}) \cdot \beta_{TEG} + (1-\beta_{TEG}) \cdot T_{g\_in1}] \cdot (\lambda_{TEG} - 1) \end{array} \quad (24)$$

Where 1, 2 are the numbers to design the first and the second row and λ, β the percentage of the gas that is actually producing and not by-passed. The other two rows are modelled following the same approach.

The effect of the backpressure on the gas side has been considered taken into account the four rows and the followed methodology is the same as in the Engine section.

Block 9: Turbo Generator

The gas inlet pressure is obtained from the expression of the coefficient of expansion in Eq.25, thanks a correlation fitting function of the exhaust gas mass flow from experimental data for a current TBG.

$$\beta_{turb} = \frac{p_{out}}{p_{in}} = a + b \cdot m_g + c \cdot m_g^2 + d \cdot m_g^3 \quad (25)$$

Where a,b,c,d are constants of this turbo-generator.

Then, the outlet gas temperature is obtained from the Eq. 26:

$$T_{gout} = T_{gin} \cdot [1 - \eta_t (1 - \beta_{turb}^{\frac{k-1}{k}})] \quad (26)$$

Where k is the polytrophic coefficient (considered = 1.391) and η the isentropic turbine efficiency obtained from a correlation validated with experimental data and function of β_{turb}^{-1}

The electrical power generated from the turbo generator is calculated from the Eq.27.

$$W_{TBG}[kW] = \eta_{turb} \cdot m_g \cdot cp_g \cdot (T_{gin\_turb} - T_{gout\_turb}) \quad (27)$$

This power is limited currently in the model by a maximum allowed back-pressure of 300mbar (including TEG and TBG) according to the engine manufacturer. Therefore, a gas mass flow by-pass controlled by the inlet pressure to do not reach the maximum drop pressure is added to this part. Therefore, all the expressions dependents to mg, include only the gas mass flow after the by-pass

Finally, the gas temperature to the ambient is calculated taken into account the by-bass according to Eq.28.

$$T_{gout\_turb} = (1 - \psi) T_{gin\_turb} + \psi \cdot T_{gin\_turb} \cdot [1 - \eta_t (1 - \beta_{turb}^{\frac{k-1}{k}})] \quad (28)$$

Where ψ is the gas mass flow rate through the TBG.